THE JOURNAL OF BIOLOGICAL CHEMISTRY VOL. 291, NO. 47, pp. 24335–24351, November 18, 2016

Lack of Heterologous Cross-reactivity toward HLA-A*02:01 Restricted Viral Epitopes Is Underpinned by Distinct αβT Cell Receptor Signatures*

Received for publication, August 15, 2016, and in revised form, September 11, 2016 Published, JBC Papers in Press, September 19, 2016, DOI 10.1074/jbc.M116.753988

Emma J. Grant[‡], Tracy M. Josephs[§¶], Sophie A. Valkenburg[‡], Linda Wooldridge[‖], Margaret Hellard[**], Jamie Rossjohn[§¶‡‡], Mandvi Bharadwaj[‡], Katherine Kedzierska[‡1,2], and Stephanie Gras[§¶1,3]

*From the [‡]Department of Microbiology and Immunology, University of Melbourne at the Peter Doherty Institute for Infection and Immunity, Parkville, Victoria 3010, Australia, the [§]Infection and Immunity Program and Department of Biochemistry and Molecular Biology, Biomedicine Discovery Institute, and the [¶]Australian Research Council Centre of Excellence for Advanced Molecular Imaging, Monash University, Clayton, Victoria 3800, Australia, the [‖]Faculty of Health Sciences, University of Bristol, Bristol BS8 1TD, United Kingdom, the **Center for Research Excellence in Injecting Drug Use, Burnet Institute, Melbourne, Victoria 3004, Australia, and the [‡‡]Institute of Infection and Immunity, Cardiff University School of Medicine, Heath Park, Cardiff CF14 4XN, United Kingdom*

αβT cell receptor (TCR) genetic diversity is outnumbered by the quantity of pathogenic epitopes to be recognized. To provide efficient protective anti-viral immunity, a single TCR ideally needs to cross-react with a multitude of pathogenic epitopes. However, the frequency, extent, and mechanisms of TCR cross-reactivity remain unclear, with conflicting results on anti-viral T cell cross-reactivity observed in humans. Namely, both the presence and lack of T cell cross-reactivity have been reported with HLA-A*02:01-restricted epitopes from the Epstein-Barr and influenza viruses (BMLF-1 and $M1_{58}$, respectively) or with the hepatitis C and influenza viruses ($NS3_{1073}$ and NA_{231}, respectively). Given the high sequence similarity of these paired viral epitopes (56 and 88%, respectively), the ubiquitous nature of the three viruses, and the high frequency of the HLA-*A*02:01* allele, we selected these epitopes to establish the extent of T cell cross-reactivity. We combined *ex vivo* and *in vitro* functional assays, single-cell αβTCR repertoire sequencing, and structural analysis of these four epitopes in complex with HLA-A*02:01 to determine whether they could lead to heterologous T cell cross-reactivity. Our data show that sequence similarity does not translate to structural mimicry of the paired epitopes in complexes with HLA-A*02:01, resulting in induction of distinct αβTCR repertoires. The differences in epitope architecture might be an obstacle for TCR recognition, explaining the lack of T cell cross-reactivity observed. In conclusion, sequence similarity does not necessarily result in structural mimicry, and despite the need for cross-reactivity, antigen-specific TCR repertoires can remain highly specific.

αβT cells recognize peptides (p) bound to the MHC molecule, or human leukocyte antigen (HLA)[4] in humans, via their αβT cell receptor (TCR). Each TCR comprises two chains, α and β, that are composed of variable (V), joining (J), and constant (C) genes for the α-chain and an additional diversity (D) segment for the β-chain. The TCR has three complementarity determining regions (CDRs), which determine pHLA specificity (1). Although CDR1 and CDR2 are germ line encoded and found within the V gene segment, the CDR3 spans the junction between the V(D)J gene segments. During somatic recombination, TCR gene segments are rearranged, and the additional insertion/deletion of nucleotides at each gene junction creates a high level of diversity within the CDR3, termed a hypervariable loop (2). Thus, the CDR3 loops are often used to define epitope-specific αβTCR clonotypes.

The clonal selection theory (3) suggests that protective immunity is a "one clonotype, one specificity" system, in which a single TCR recognizes a single pHLA complex. However, this theory was questioned by Mason (4), who hypothesized that 10^{15} T cells would be required to recognize 10^{15} non-self peptides. Because the weight of 10^{15} T cells would be more than 500 kg in one individual, such single specificity of T cells is mathematically impossible. This suggests that each T cell must be able to recognize a vast number of peptides to ensure protective immunity in a process known as cross-reactivity. Thus, T cell cross-reactivity is critical for the efficacy of the immune system,

* This work was supported by Australian NHMRC Project Grant AI1008854 and Program Grant AI1071916 (to K. K.), an NHMRC Aboriginal and Torres Strait Islander Health Research Scholarship (to E. J. G.), a Douglas and Lola Douglas Scholarship in Medical Science (to E. J. G.), an NHMRC C. J. Martin Fellowship (to E. J. G.), NHMRC Australia Fellowship AF50 (to J. R.), Australian Research Council (ARC) Future Fellowship FF120100416 (to S. G.), and an NHMRC Senior Research Fellow level B (SRFB) Fellowship (to K. K.). The authors declare that they have no conflicts of interest with the contents of this article.

The atomic coordinates and structure factors (code 5SWQ) have been deposited in the Protein Data Bank (http://wwpdb.org/).

[1] Both authors contributed equally to this work.

[2] To whom correspondence may be addressed: Dept. of Microbiology and Immunology, University of Melbourne, Peter Doherty Institute for Infection and Immunity, Parkville, Victoria 3010, Australia. Tel.: 613-8344-7962; Fax: 613-9347-1540; E-mail: kkedz@unimelb.edu.au.

[3] To whom correspondence may be addressed: Infection and Immunity Program and Dept. of Biochemistry and Molecular Biology, Biomedicine Discovery Institute, Monash University, Clayton, Victoria 3800, Australia. Tel.: 613-9905-0254; E-mail: Stephanie.Gras@monash.edu.

[4] The abbreviations used are: HLA, human leukocyte antigen; TCR, T cell receptor; PDB, Protein Data Bank; EBV, Epstein-Barr virus; HCV, hepatitis C virus; NHMRC, National Health and Medical Research Council; CDR, complementarity determining region; LCMV, lymphocytic choriomeningitis virus; VV, vaccinia virus; P*n*, position *n*; aa, amino acid(s); PBMC, peripheral blood mononuclear cell; ICS, intracellular cytokine staining; PFA, paraformaldehyde; APC, antigen presenting cell; PE, Phycoerythrin.

whereby T cells exposed to one epitope can recognize viral variants (5–7) to provide immune protection upon subsequent challenge (5).

T cell cross-reactivity can also occur during viral infections, in which effector or memory CD8$^+$ T cells can recognize epitopes from an unrelated virus, a process known as heterologous T cell cross-reactivity. Heterologous T cell cross-reactivity has been extensively characterized in murine models, in which mice primed with one virus can be subsequently challenged with an unrelated virus during the effector phase (8–12). Studies using similar viruses, such as lymphocytic choriomeningitis virus (LCMV) and Pichinde virus (9), or distinct viruses, such as LCMV and vaccinia virus (VV) (10), have shed some light onto the mechanisms of heterologous cross-reactivity. For example, the H-2K^b-restricted NP$_{205}$ epitope from both LCMV (**YTVK**Y**PN**L) and Pichinde virus (**YTVK**F**PN**M) are 75% identical, with differences only at position (P) 5 and P8 (9). Structures of the two H-2K^b-NP$_{205}$ peptides revealed that P5 and P8, which share similar residues, were both buried inside the antigen-binding cleft, thereby enabling a high level of cross-reactivity toward these distinct viral peptides. Conversely, others have shown that heterologous cross-reactivity can occur toward epitopes with lower sequence identity. For example, the LCMV gp$_{34}$ epitope (**A**VY**N**F**A**TM) and the VV A11R$_{198}$ epitope (**AI**V**N**Y**A**NL) share three identical residues (37% identity). However, previous exposure to LCMV provided a level of protection against VV (13). Despite sharing only three identical residues, the two pMHC complexes adopted similar structures, with the variable amino acids buried within the antigen-binding cleft, thus providing a molecular basis for T cell cross-reactivity (14).

A recent study utilizing a library of peptides containing systematic substitutions showed that TCRs are predominantly cross-reactive because they are tolerant of peptide residue substitutions rather than recognizing multiple distinct peptides (14). Moreover, the "tolerated" substitutions were either not in direct contact with the TCR or were conservative and thus permitted binding by the TCR, in line with the observations from Shen *et al.* (13). This suggests that T cells can cross-recognize distinct pMHC complexes because they are permissive of substitutions and recognize specific pMHC architectures rather than degeneracy in TCR binding. Accordingly, only a handful of studies have shown how a single $\alpha\beta$TCR could engage highly divergent pMHC complexes (15–18).

Although heterologous immunity in mice is well established, there is controversy regarding heterologous T cell cross-reactivity in humans and its impact on protective anti-viral immunity. For example, studies have described the presence (19, 20) or absence (21) of heterologous CD8$^+$ T cell cross-reactivity toward the HLA-A*02:01-restricted influenza-derived (M1$_{58}$, **G**ILGF**V**FT**L**) and Epstein-Barr virus (EBV)-derived (BMLF-1, **G**LCTL**V**AM**L**) epitopes. Similarly, other studies have described the presence (22–24) or absence (25, 26) of heterologous CD8$^+$ T cell cross-reactivity toward the HLA-A*02:01-restricted influenza-derived (NA$_{231}$, **CVNGS**C**FTV**) and hepatitis C virus (HCV)-derived (NS3$_{1073}$, **CINGV**C**WTV**) epitopes. Interestingly, both NS3$_{1073}$ and NA$_{231}$ epitopes exhibit variations between distinct viral strains, which may explain the variable frequency of cross-reactivity between individuals (22, 26), because a single amino acid substitution can impact the CD8$^+$ T cell frequency and cross-reactivity (27).

Based on the previous reports of human heterologous cross-reactivity (20, 23, 24, 28), we focused our current study on the well described and highly prevalent HLA-A*02:01-restricted epitopes, namely M1$_{58}$/BMLF-1 and NS3$_{1073}$/NA$_{231}$. These paired peptides share identical (3 and 6, respectively) as well as chemically conserved (2 each) residues, with a sequence homology of 56 and 88%, respectively. Therefore, they provide a good model to determine the molecular basis underlying heterologous T cell cross-reactivity in humans.

In this study, we combined single-cell $\alpha\beta$TCR repertoire sequencing with biophysical and structural analysis of the four epitopes in complex with the HLA-A*02:01 molecule. We also undertook functional studies (including *ex vivo* and *in vivo* T cell expansion in healthy individuals for both peptide pairs and in HCV-infected individuals for the NS3$_{1073}$/NA$_{231}$ peptide pair) to determine the frequency and biological relevance of heterologous T cell cross-reactivity toward these HLA-A*02:01-restricted epitopes. Our data show that the sequence similarity between the paired epitopes did not translate to structural mimicry. Namely, the paired epitopes exhibited distinct architectures and mobility within the HLA binding cleft and selected distinct $\alpha\beta$TCR repertoires. Together, these findings underlie a lack of heterologous cross-reactivity detected directly *ex vivo* by tetramer enrichment and *in vitro* via IFN-γ and tetramer assays. Whereas T cell cross-reactivity is an intrinsic requirement for protective immunity, our data indicate that the sequence similarity of peptides alone is not a reliable indication of CD8$^+$ T cell cross-reactivity. In line with previous studies (13, 14), our results highlight that pHLA architecture impacts CD8$^+$ T cell cross-reactivity.

Results

Lack of Structural Homology between Paired Epitopes—To understand the mechanisms underpinning human heterologous CD8$^+$ T cell cross-reactivity, we selected two pairs of prominent human epitopes containing viral peptides derived from three ubiquitous viruses (influenza, HCV, and EBV) that display high sequence similarity and are restricted by HLA-A*02:01. Conflicting literature reports either the presence (20, 23, 24) or lack (21, 25, 26) of heterologous CD8$^+$ T cell cross-reactivity between HLA-A*02:01-restricted epitopes M1$_{58}$ (GILGFVFTL) and BMLF-1 (GLCTLVAML) epitopes, as well as NA$_{231}$ (CVNGSCFTV) and NS3$_{1073}$ (CINGVCWTV).

The M1$_{58}$ and BMLF-1 epitopes share 56% sequence homology, with three identical residues at P1-Gly, P6-Val, and P9-Leu (similarly to the LCMV gp$_{34}$ and VV A11R$_{198}$ epitopes), as well as chemically conserved P2-I/L and P5-F/L residues. The NA$_{231}$ and NS3$_{1073}$ peptides share higher sequence homology (88%). To determine whether the sequence variation could impact the stability of each peptide within the HLA-A*02:01 antigen binding cleft, we performed a thermal stability assay. The thermal melting point (T_m) values were very similar for the paired pHLA complexes, with a T_m of ~59 °C for M1$_{58}$ and BMLF-1 and of ~56 °C for NA$_{231}$ and NS3$_{1073}$, suggesting that each pHLA complex displays similar stability.

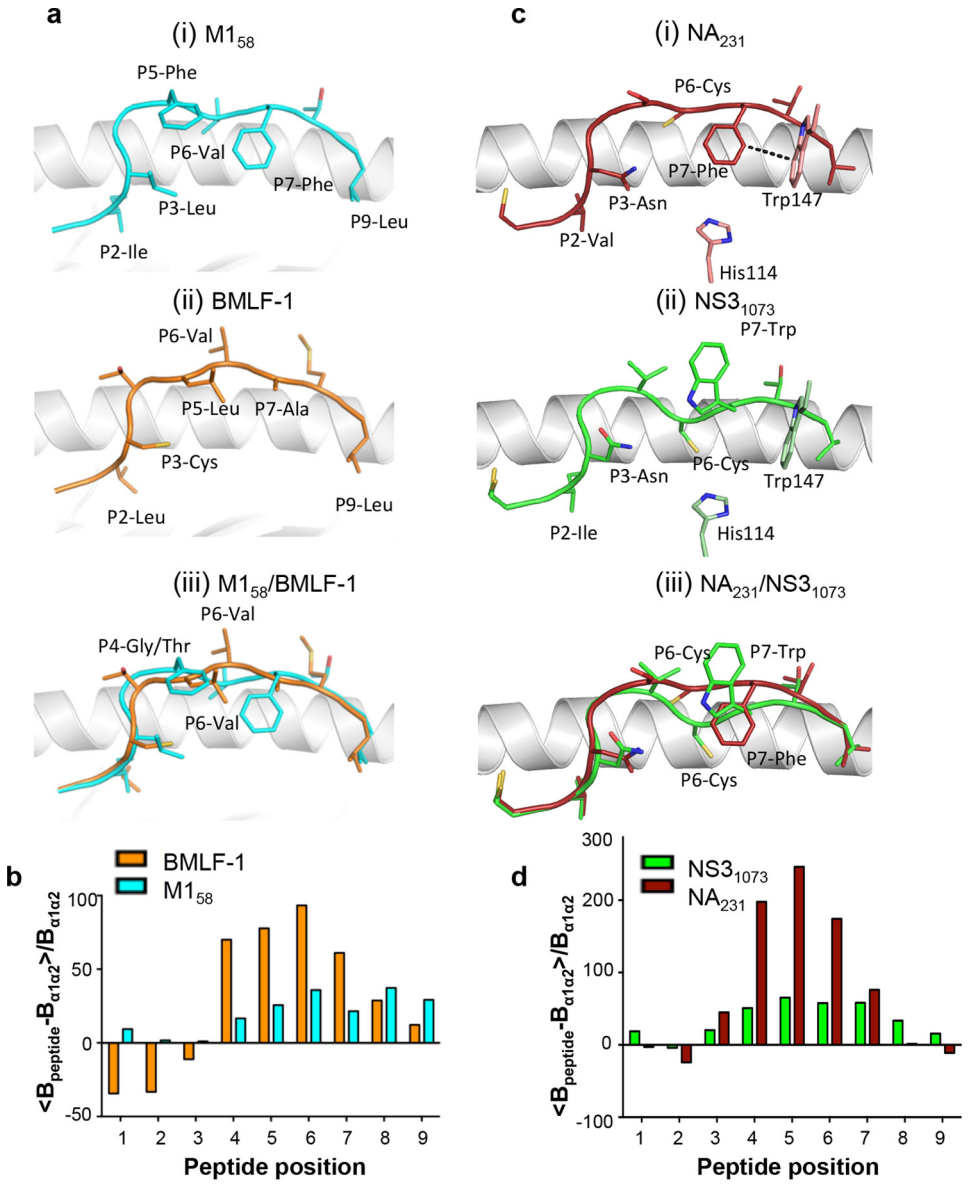

FIGURE 1. **Structural differences between peptide pairs bound to the HLA-A*02:01 molecule.** The panels represent the HLA-A*02:01 cleft in *white cartoon*, bound to the four different peptides in *stick format*. *a*, structures of the M1$_{58}$ peptide in *cyan* (*panel i*), BMLF-1 in *orange* (*panel ii*), and a superposition of the two peptides in complex with HLA-A*02:01 (*panel iii*). *b*, histogram of the relative mean B factors for the M1$_{58}$ (*cyan*) and BMLF-1 (*orange*) peptides. For each peptide residue, $100 \times ((<B_{residue}> - <B_{HLA\text{-}A*02:01\text{-}\alpha1\alpha2}>)/<B_{HLA\text{-}A*02:01\text{-}\alpha1\alpha2}>)$ was calculated, with positive values representing a peptide residue more mobile than the overall HLA $\alpha1\alpha2$ domains, and negative values representing a peptide residue more stable. *c*, structures of the NA$_{231}$ peptide in brown (*panel i*), NS3$_{1073}$ in *green* (*panel ii*), and a superposition of the two peptides in complex with HLA-A*02:01 (*panel iii*). *d*, histogram of the relative mean B factors for the NA$_{231}$ (*brown*) and NS3$_{1073}$ (*green*) peptides, calculated as per *B*.

We next compared the four peptide-HLA-A*02:01 structures (Fig. 1). The structures of HLA-A*02:01 in complex with NS3$_{1073}$ (PDB code 3MRG (27)), BMLF-1 (PDB code 3MRE (27)), and M1$_{58}$ (PDB code 2VLL (29)) were determined previously, and here we report the HLA-A*02:01-NA$_{231}$ structure to a resolution of 2.0 Å (Table 1). The four pHLA complexes adopted similar overall structures, with an average root mean standard deviation of 0.40 Å on the Cα atoms of the $\alpha1\alpha2$ domains. All four peptides adopted an extended conformation within the HLA-A*02:01 cleft, whereby the P2 and P9 residues were used as anchors and were buried inside the cleft, whereas P3 acted as a partial anchor residue.

*Structure of M1$_{58}$ versus BMLF-1 in Complex with HLA-A*02:01*—The M1$_{58}$ peptide has been referred to as a "plain vanilla" peptide, because its structure is featureless in the cleft of HLA-A*02:01; the two large Phe residues at P5 and P7 are buried inside the cleft, and only the small P6-Val side chain is exposed for TCR contact (Fig. 1*a*, *panel i*) (29–31). The P5-Leu and P7-Ala of the BMLF-1 peptide (27) adopted a buried conformation similar to the P5 and P7 of the M1$_{58}$ epitope (Fig. 1*a*, *panel ii*); however, the smaller P5 and P7 side chains of the BMLF-1 peptide were shifted toward the HLA $\alpha2$-helix. As a result, the conserved P6-Val adopted a more central and fully solvent-exposed conformation in the BMLF-1 peptide than in the M1$_{58}$ peptide (Cα displacement of 1.6 Å; Fig. 1*a*, *panel iii*).

TABLE 1
Data collection and refinement statistics

	HLA-A*02:01-NA_{231}
Data collection statistics	
Temperature (K)	100
Space group	$P2_1$
Cell dimensions	
a, *b*, *c* (Å)	51.45, 80.06, 55.00
β (°)	111.36
Resolution (Å)	100–2.00 (2.10–2.00)
Total number of observations	87,946 (11,254)
Number of unique observations	26,350 (3398)
Multiplicity	3.3 (3.3)
Data completeness (%)	93.5 (89.4)
$I/\sigma I$	11.18 (3.57)
R_{merge} (%)[a]	10.0 (39.0)
Refinement statistics	
Non-hydrogen atoms	
Protein	3259
Water	372
R_{factor} (%)[b]	19.4
R_{free} (%)[b]	25.8
Root mean square deviations from ideality	
Bond lengths (Å)	0.008
Bond angles (°)	1.165
Ramachandran plot (%)	
Favored	98.48
Outliers	0

[a] $R_{merge} = \Sigma|I_{hkl} - <I_{hkl}>|/\Sigma I_{hkl}$.
[b] $R_{factor} = \Sigma_{hkl}||F_o| - |F_c||/\Sigma_{hkl}|F_o|$ for all data except ≈5%, which were used for R_{free} calculation. The values in parentheses are for the highest resolution shell.

Moreover, as judged by temperature factor analyses (relative B factor of each peptide residue compared with the HLA antigen binding cleft B factor), the central part (P4–P7) of the BMLF-1 peptide was more flexible than the $M1_{58}$ peptide, with a maximum mobility at the conserved P6-Val (Fig. 1*b*). Peptide mobility can influence peptide conformation, as well as CD8$^+$ T cell recognition (32, 33). Therefore, despite a conserved P6-Val and 56% sequence homology, the $M1_{58}$ and BMLF-1 peptides were presented differently by the HLA-A*02:01 molecule.

*Structure of NA_{231} versus $NS3_{1073}$ in Complex with HLA-A*02:01*—Despite the sequence similarity of the NA_{231} and $NS3_{1073}$ epitopes (27), the structures of both peptides differed (Fig. 1*c*). For example, the conserved aromatic residue at P7 ($NS3_{1073}$ P7-Trp; NA_{231} P7-Phe) adopted contrasting conformations. The NA_{231} P7-Phe was buried inside the cleft and interacted with Trp^{147} and His^{114} of HLA-A*02:01 (Fig. 1*c*, *panel i*) and was not available for TCR recognition. Conversely, the $NS3_{1073}$ P7-Trp was solvent-exposed, with its aromatic side chain potentially available for TCR interaction (Fig. 1*c*, *panel ii*). The different P7 conformations changed the central part of the peptide (Fig. 1*c*, *panel iii*), resulting in the conserved P6-Cys sitting higher in the HLA-A*02:01 cleft for the NA_{231} peptide compared with $NS3_{1073}$ (Cα deviation of 2.4 Å). This resulted in a 20% decrease in TCR accessible surface area for the NA_{231} peptide (270 Å^2) compared with $NS3_{1073}$ (335 Å^2) (Fig. 1*c*, *panel iii*). Temperature factor analysis revealed that the $NS3_{1073}$ peptide was rigid, whereas the NA_{231} peptide showed higher mobility at P4 to P6 (Fig. 1*d*). Taken together, the structural analysis revealed that HLA-A*02:01 presents the two peptide pairs with distinct epitope conformations and differing flexibility.

CD8$^+$ T Cells Utilize Distinct $\alpha\beta$TCR Repertoires to Recognize the Epitopes Pairs—Next, we asked whether the responding $\alpha\beta$TCR repertoires showed any overlap in response to the paired HLA-A*02:01-restricted $M1_{58}$/BMLF-1 and $NS3_{1073}$/NA_{231} epitopes. We investigated the $\alpha\beta$TCR clonotypes (Fig. 2) and CDR3$\alpha\beta$ usage (Fig. 3) in $M1_{58}$- and BMLF-1-reactive CD8$^+$ T cell lines (Fig. 2*a*) or in $NA_{231}{}^+$CD8$^+$ and $NS3_{1073}{}^+$CD8$^+$ T cells generated directly *ex vivo* from healthy donors following tetramer magnetic enrichment (Fig. 2*b*). In addition, we assessed the recognition of $NS3_{1073}$ by CD8$^+$ T cell lines from donors with chronic HCV infection (Fig. 2*c*). CD8$^+$tetramer$^+$ cells were single cell-sorted, and the $\alpha\beta$TCR repertoire was determined using human RT-PCR multiplex (34).

The $M1_{58}$-specific $\alpha\beta$TCR repertoire was quite diverse in the three donors (12–19 clonotypes/donor from 27–32 sequences). The $M1_{58}$-specific $\alpha\beta$TCR clonotypes were highly biased toward TRBV19 gene usage (96.3 ± 3.7%) and paired with different TRAV chains (Table 2 and Fig. 2*a*, *panel i*), in line with previously published repertoires (35, 36). Distinct $M1_{58}$ clonotypes favored a CDR3α length of 9 amino acids (aa) (29.9 ± 17.4%) (Fig. 3*a*, *panel i*) and a short CDR3β of 8 aa (74.6 ± 0.8%) (Fig. 3*a*, *panel ii*). Multiple CDR3α sequences were observed (GGSQGNL, GGTSYGKL, and SSNTGKL) (Table 2) sharing the $Z_{3-4}XG$ motif (Fig. 3*b*, *panel i*), where *Z* represents a small amino acid (Gly, Ser, or Thr), and *X* represents any residue, irrespective of the TRAV gene pairing. This motif is known to allow the CDR3α loop to closely contact P4-P5 of the peptide (31). The common CDR3β RS motif was detected in 28, 63, and 74% of total sequences from donors H-1, H-2, and H-3, respectively (Table 2 and Fig. 3*b*, *panel i*), consistent with previously published data (30, 35, 36).

The BMLF-1-specific $\alpha\beta$TCR repertoire was relatively more restricted (5–7 clonotypes/donor from 27–32 sequences) (Table 2; Fig. 2*a*, *panel ii*). A bias for the TRAV5/TRBV20 pairing was observed in all donors (100, 9.7, and 40.7% in H-1, H-2, and H-3 donors, respectively) (Table 2), consistent with previously published data (37). Furthermore, the same CDR3α loop sequence (DNNARL) was observed in the H-1 donor (84%) and the H-3 donor (4%), with conserved sequences found in donor H-2 (D(S/Q)NARL, 9%) (Table 2). The distinct CD8$^+$ T cell clonotypes from the three donors preferred a short CDR3α of 6 aa (48.4 ± 45.1%) (Fig. 3*a*, *panel i*) with a conserved D*X*NARL motif (Fig. 3*b*, *panel ii*) and a preferred an 8-aa-long CDR3β (63.5 ± 33.8%) (Fig. 3*a*, *panel ii*) exhibiting shared motif (R*XXX*GN, Fig. 3*b*, *panel ii*).

There were no evident TRAV or TRBV biases in the NA_{231}-specific CD8$^+$ T cells (Table 3 and Fig. 2*b*, *panel i*). The most common CDR3α lengths for the distinct clonotypes were 8 or 10 aa (both 28.3 ± 10.4%) (Fig. 3*a*, *panel i*), whereas CDR3β was most commonly 10 aa long (26.7 ± 30.6%) (Fig. 3*a*, *panel ii*). No shared motifs were observed within either of the CDR3 loops (Fig. 3*b*, *panel iii*). The number of NA_{231}-specific TCRs available was low because of their low pHLA affinity and the predominant naïve phenotype of the NA_{231}-specific CD8$^+$ T cells.

The $NS3_{1073}$ TCR$\alpha\beta$ repertoire was characterized by a limited TCR$\alpha\beta$ diversity in donors with chronic HCV infection. HCV-1 had seven $NS3_{1073}$-specific clonotypes, whereas HCV-2 had a more limited repertoire with only four clonotypes (Fig. 2*c*). A TRAV4 bias was observed in the TCR repertoire of both healthy (37.8 ± 20.4%) and HCV-infected donors (59.1 ±

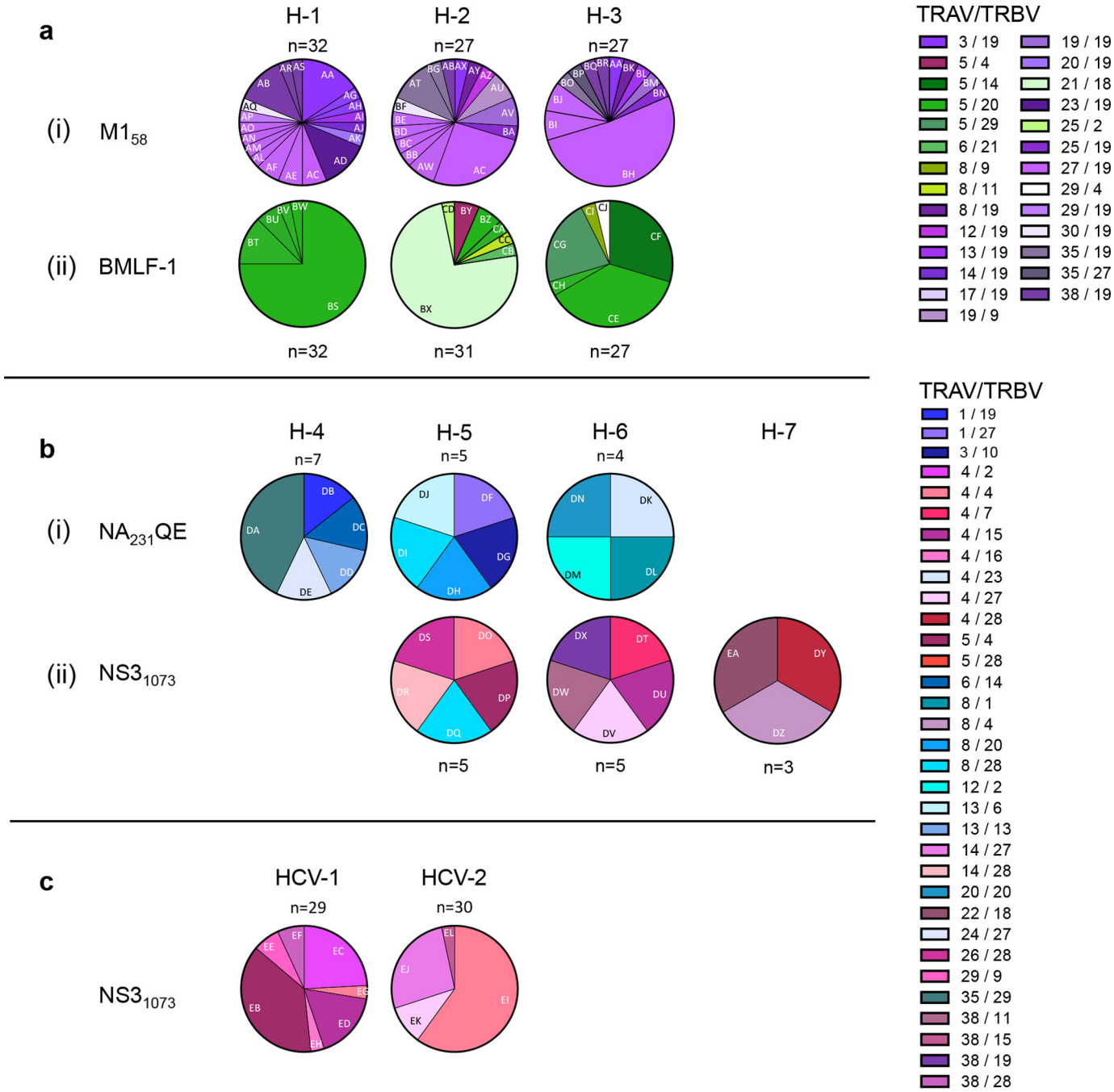

FIGURE 2. **Distinct $\alpha\beta$TCR repertoires recognize each peptide in complex HLA-A*02:01.** PBMCs from healthy and HCV-infected donors were stimulated with the M1$_{58}$ or BMLF-1 peptides (13 days) or the NS3$_{1073}$ peptide (19–21 days). CD8$^+$ T cell lines were stained with the cognate peptide, whereas PBMCs (from healthy donors) were stained with either NA$_{231}$QE or NS3$_{1073}$ tetramers and were magnetically enriched. The cells were stained as lymphocytes, singlets, CD3$^{mid\text{-}high}$, dump$^-$ (PBMCs only), CD8$^+$, tetramer$^+$ cells, and single-cell sorted. Then the $\alpha\beta$TCR repertories were determined using a multiplex RT-PCR. *a*, $\alpha\beta$TCR repertoire utilized to recognize the M1$_{58}$ (*panel i*) or BMLF-1 (*panel ii*) tetramers (in H-1, H-2, and H-3 healthy donors). *b*, $\alpha\beta$TCR repertoire utilized to recognize NA$_{231}$QE (*panel i*) or NS3$_{1073}$ (*panel ii*) tetramers (in H-4, H-5, H-6, and H-7 healthy donors). *c*, NS3$_{1073}$ tetramer$^+$ $\alpha\beta$TCR repertoire (HCV1 and HCV-2 are HCV-infected donors).

15.4%), which paired with a range of TRBVs (Fig. 2, *b* and *c*), despite the low number of NS3$_{1073}$-specific CD8$^+$ T cells isolated from healthy donors because of their predominant naïve phenotype. In addition, the HCV-1 donor showed a preference for TRAV5 (~38%) (Fig. 2*c*). The NS3$_{1073}$-reactive repertoire from both healthy and HCV-infected individuals consisted of distinct clonotypes with different CDR3 lengths, with the most common CDR3α length of 10 aa (26.4 ± 18.4%) (Fig. 3*a*, *panel i*) and the most common CDR3β length of 9 aa (26.3 ± 24.5%) (Fig. 3*a*, *panel ii*).

Overall, no common TCR$\alpha\beta$ clonotypes were utilized for the recognition of M1$_{58}$ and BMLF-1 or the NA$_{231}$ and NS3$_{1073}$ peptides. On a broader level, only a single common TRAV8/TRBV28 pair was identified in the NA$_{231}$ and NS3$_{1073}$ TCR$\alpha\beta$ repertoires; however, they were completely distinct clonotypes. Furthermore, no common TRAV/TRBV pairs were detected in

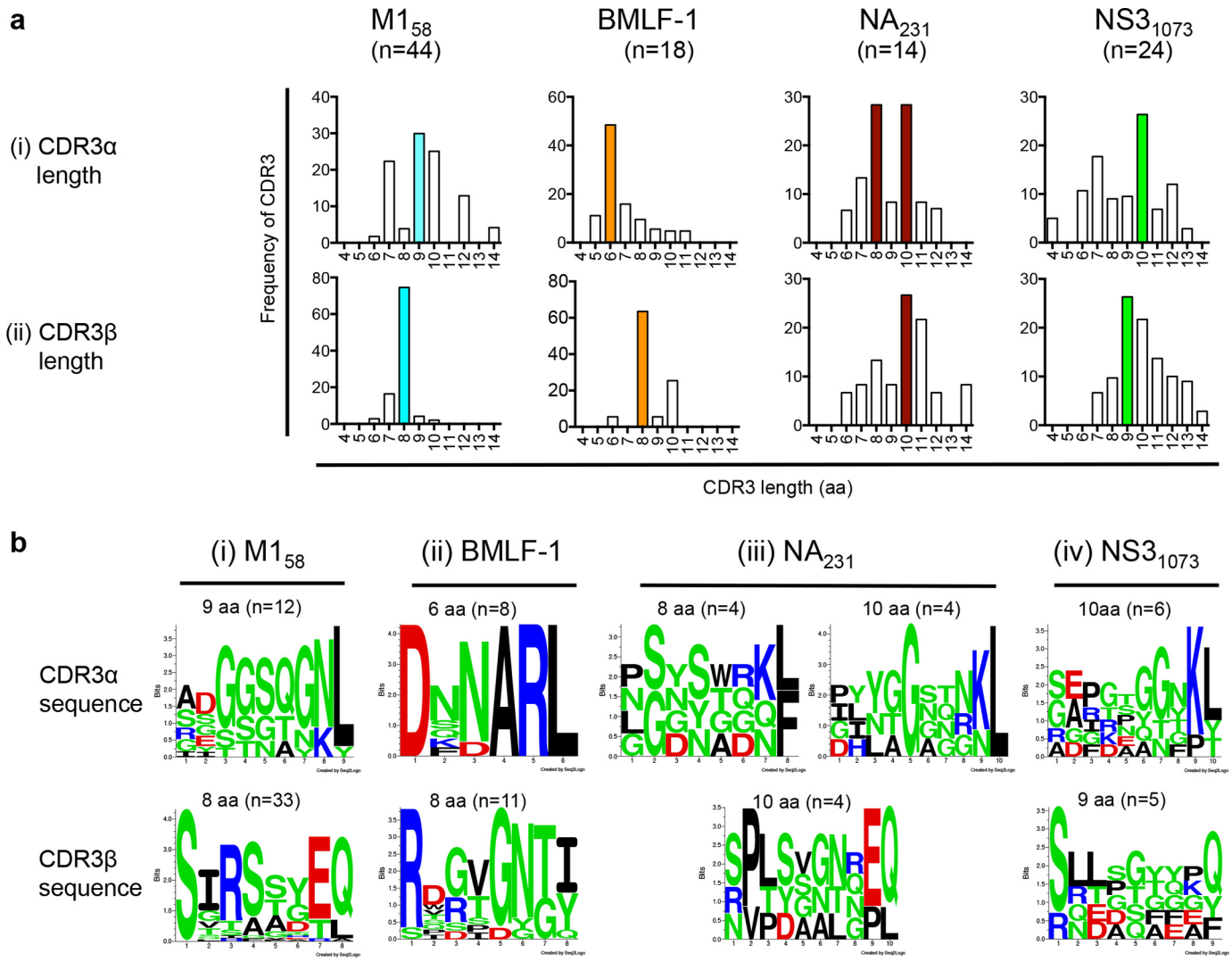

FIGURE 3. **Epitope-specific CDR3$\alpha\beta$ motifs are conserved between donors.** *a*, CDR3α (*panel i*) and CDR3β (*panel ii*) length used by distinct antigen-specific CD8$^+$ T cell clonotypes for recognition of M1$_{58}$ (*cyan*), BMLF-1 (*orange*), NA$_{231}$ (*brown*), and NS3$_{1073}$ (*green*) peptides. The *colored bar* represents the most frequent CDR3 length for each peptide. *b*, analysis of the CDR3 motifs (of the most common lengths) used by distinct clonotypes in the recognition of M1$_{58}$ (*panel i*), BMLF-1 (*panel ii*), NA$_{231}$ (*panel iii*), and NS3$_{1073}$ (*panel iv*). *n* = number of distinct clonotypes.

the M1$_{58}$ and BMLF-1 $\alpha\beta$TCR repertoires. These findings further highlight the high level specificity of memory CD8$^+$ T cells for their pHLA. Thus, despite high sequence homology, the paired peptides were structurally different and mobilized distinct $\alpha\beta$TCR repertoires with no overlap.

*Lack of T Cell Cross-reactivity Observed for the Paired HLA-A*02:01-restricted Epitopes as Assessed Directly ex Vivo*—Based on our findings on differing $\alpha\beta$TCR repertoires, we next investigated heterologous cross-reactivity directly *ex vivo* from human peripheral blood mononuclear cells (PBMCs). We used a magnetic enrichment technique (38, 39) for an unbiased detection of low-frequency epitope-specific CD8$^+$ T cells. PBMCs from healthy HLA-*A*02:01*-positive donors were stained with the specific HLA-*A*02:01*$^+$ tetramer, positively enriched, and surface-stained using αCD3, αCD8, dump (αCD4, αCD14, and αCD19), and phenotypic antibodies (Fig. 4*a*). Using the phenotypic antibodies CD27 and CD45RA, M1$_{58}$- and NS3$_{1073}$-specific CD8$^+$ T cells from healthy donors were analyzed for their activation phenotype, respectively (Fig. 4*b*). Furthermore, using the CD8α enhanced (40) HLA-*A*02:01*-Q115E-NA$_{231}$ mutant tetramer (NA$_{231}$QE), we detected low affinity NA$_{231}$-specific CD8$^+$ T cells, which were undetectable with the WT tetramer (Fig. 4*c*). We identified memory M1$_{58}$- and BMLF-1-specific CD8$^+$ T cells across donors with a mean frequency of 5×10^{-5} and 1×10^{-4}, respectively (Fig. 4*d*). Low affinity NA$_{231}$- and naïve CD27$^+$CD45RA$^+$ NS3$_{1073}$-specific CD8$^+$ T cells were found at lower frequencies comparable with other studies (39), at 3×10^{-6} and 4×10^{-6}, respectively (Fig. 4*d*).

To identify any cross-reactive CD8$^+$ T cells directly *ex vivo*, PBMCs from healthy and HCV$^+$ donors (Table 4) were co-stained with either M1$_{58}$ and BMLF-1 or NA$_{231}$QE and NS3$_{1073}$ tetramers conjugated to different fluorochromes, followed by tetramer magnetic enrichment (Fig. 5). Memory M1$_{58}^+$- and BMLF-1$^+$-specific CD8$^+$ T cell populations were detected at an average of 12.0 ± 7.8 and 20.4 ± 16.1% of CD8$^+$ T cells, respectively (Fig. 5*b*, *panel i*). Similarly, naïve NS3$_{1073}$- and low affinity NA$_{231}$-specific CD8$^+$ T cells were detected in healthy donors

TABLE 2

$\alpha\beta$TCR repertoire usage for the recognition of $M1_{58}$ and BMLF-1

Code represents the individual clonotypes. The colored residues represent the conserved motifs within the CDR3 loops between donors, in which blue is the $Z_{3-4}XG$ motif (Z is a small amino acid, and X is any residue), red is the RS motif of the $M1_{58}$-specific clones, purple is the D*X*NARL motif, and green is the R*XXX*GN motif of the BMLF-1-specific clones. Each clonotype frequency is expressed as the proportion of total sequences. TRAV, variable α-chain gene usage; TRBV, β-chain gene usage; TRAJ, junction α-chain gene usage; TRBJ, junction β-chain gene usage; H, individual donor.

								Frequency $M1_{58}$		
Code	**Pairs**	**TRAV**	**TRAJ**	**CDR3α**	**TRBV**	**TRBJ**	**CDR3β**	**H-1**	**H-2**	**H-3**
AA	3/19	3	36	CAV-RDGTGANNL-FF	19	2-2	CAS-SISSTGEL-FF	16		4
AB	38-1/19	38-1	52	CAF-MKDAGGTSYGKL-TF	19	1-2	CAS-SIGVYGY-TF	13	4	
AC	27/19	27	42	CAG-GGSQGNL-IF	19	2-7	CAS-SIRSSYEQ-YF	6	26	
AD	23/19	23/DV6	42	CAL-AGSQGNL-IF	19	2-7	CAS-SIRASYEQ-YF	13		
AE	27/19	27	42	CAG-ADGGSQGNL-IF	19	2-2	CAS-SGRAAGEL-FF	6		
AF	27/19	27	42	CAA-GGSQGNL-IF	19	2-7	CAS-SVRSSYEQ-YF	6		
AG	3/19	3	37	CAA-PPSNTGKL-IF	19	2-3	CAS-STRAADTQ-YF	3		
AH	3/19	3	27	CAV-RDLLTNAGKS-TF	19	2-7	CAS-SGTSGTEQ-YF	3		
AI	13-2/19	13-2	42	CAE-NMGGGSQGNL-IF	19	2-5	CAS-SIRAGETQ-YF	3		
AJ	14/19	14/DV4	42	CAM-RDGGGSQGNL-IF	19	2-7	CAS-SIRSGAEQ-YF	3		
AK	20/19	20	35	CAV-APTGNVL-HC	19	2-2	CAS-SIRSTGEL-FF	3		
AL	27/19	27	42	CAG-AGSQGNL-IF	19	2-7	CAS-SVRSSYEQ-YF	3		
AM	27/19	27	42	CAG-GLGGGSQGNL-IF	19	2-7	CAS-SIRAAYEQ-YF	3		
AN	27/19	27	42	CAG-ADGGSQGNL-IF	19	2-2	CAS-SISSTGEL-FF	3		
AO	27/19	27	37	CAG-GGSSNTGKL-IF	19	2-7	CAS-SIRSSYEQ-YF	3		
AP	29/19	29/DV5	42	CPG-GSQGNL-IF	19	1-2	CAS-SIGVYGY-TF	3		
AQ	30/19	30	42	CGT-GGSQGNL-IF	19	2-3	CSS-VRSADTQ-YF	3		
AR	38-1/19	38-1	52	CAF-MINAGGTSYGKL-TF	19	1-2	CAS-SIGSYGY-TF	3		
AS	38-2/19	38-2/DV8	52	CAY-GTNAGGTSYGKL-TF	19	1-2	CAS-SIGVYGY-TF	3		
AT	35/19	35	42	CAG-PTHDMNYGGSQGNL-IF	19	2-3	CAS-SIHSTDTQ-YF		11	
AU	19/9	19	52	CAL-SEVSNAGGTSYGKL-TF	9	2-1	CAS-SVDGGGLDEQ-FF		7	
AV	19/19	19	23	CAL-FGGYNQGGKL-IF	19	1-1	CAS-STSGGGTEA-FF		7	
AW	27/19	27	37	CAG-GGSSNTGKL-IF	19	2-7	CAS-SIRSAYEQ-YF		7	
AX	3/19	3	36	CAV-RDGTGANNL-FF	19	2-7	CAS-SGTSVHEQ-YF		4	
AY	8-6/19	8-6	42	CAV-GGSQGNL-IF	19	2-7	CAS-SIRSSYEQ-YF		4	
AZ	12-2/19	12-2	37	CAV-PPSNTGKL-IF	19	2-3	CAS-STRSADTQ-YF		4	
BA	25/19	25	42	CAG-SSGGSQGNL-IF	19	2-3	CAS-SIRSSDTQ-YF		4	
BB	27/19	27	37	CAG-AQGSSNTGKL-IF	19	2-1	CAS-SIRSAYEQ-FF		4	
BC	27/19	27	37	CAG-AVGSSNTGKL-IF	19	2-7	CAS-SIRSSYEQ-YF		4	
BD	27/19	27	37	CAG-ASSSSNTGKL-IF	19	2-7	CAS-SIRSAYEQ-YF		4	
BE	27/19	27	42	CAA-GGSQGNL-IF	19	2-7	CAS-SIRSSYEQ-YF		4	
BF	30/19	30	42	CGT-EEGGGSQGNL-IF	19	2-3	CAS-SSRSTDTQ-YF		4	
BG	35/19	35	42	CAG-RPEVDSQGNL-IF	19	2-7	CAS-SIFSVSNEQ-YF		4	
BH	27/19	27	42	CAG-AEGGSQGNL-IF	19	2-2	CAS-SIRSTGEL-FF			52
BI	27/19	27	42	CAG-AEGGSQGNL-IF	19	2-2	CAS-SGRSTGEL-FF			7
BJ	27/19	27	42	CAG-GGSQGNL-IF	19	2-7	CAS-STRSSYEQ-YF			7
BK	8 / 19	8-1	8	LKE-NTGFQKL-VF	19	2-7	CAS-SGTGAGEQ-YF			4
BL	13-2/19	13-2	42	CAE-NRGGGSQGNL-IF	19	2-7	CAS-SQRASYEQ-YF			4
BM	19/19	19	40	CAL-IITSGTYKY-IF	19	1-5	CAS-SVGQPQ-HF			4
BN	25/19	25	42	CAG-SSGGSQGNL-IF	19	2-1	CAS-SIRSTNEQ-FF			4
BO	35/19	35	42	CAG-SYGGSQGNL-IF	19	2-1	CAS-SVRSSGEQ-FF			4
BP	35/27	35	37	CAG-PDGSSNTGKL-IF	27	1-1	CAS-SLIFPGRA-FF			4
BQ	38-1/19	38-1	52	CAF-MVNAGGTSYGKL-TF	19	1-2	CAS-SIGSYGY-TF			4
BR	38-2/19	38-2/DV8	52	CAY-SPASGGTSYGKL-TF	19	1-2	CAS-SIGLYGY-TF			4
							Total # sequences	**32**	**27**	**27**

TABLE 2—*continued*

								Frequency BMLF-1		
Code	**Pairs**	**TRAV**	**TRAJ**	**CDR3α**	**TRBV**	**TRBJ**	**CDR3β**	**H-1**	**H-2**	**H-3**
BS	5 / 20	5	31	CAE-DNNARL-MF	20-1	1-3	CSA-RVGVGNTI-YF	75		
BT	5 / 20	5	31	CAE-DFNARL-MF	20-1	1-3	CSA-RTGVGNTI-YF	13		
BU	5 / 20	5	31	CAE-DNNARL-MF	20-1	1-2	CSA-RDRTGNGY-TF	6		
BV	5 / 20	5	31	CAE-DNNARL-MF	20-1	1-2	CSA-RDGTGNGY-TF	3		
BW	5 / 20	5	31	CAE-DKDARL-MF	20-1	1-3	CSA-RDRIGNTI-YF	3		
BX	21 / 18	21	41	CAL-YSNSGYAL-NF	18	1-2	CAS-RPDSDYGY-TF		74	
BY	5 / 4	5	24	CAD-GSGTTDSWGKL-QF	4-1	1-1	CAS-SQNQDMGTEA-FF		6	
BZ	5 / 20	5	31	CAE-DSNARL-MF	20-1	1-3	CSA-RSGVGNTI-YF		6	
CA	5 / 20	5	31	CAE-DQNARL-MF	20-1	1-3	CSA-RWGVGNTI-YF		3	
CB	6 / 21	6	3	CAL-DSTYSSASKI-IF	20-1	1-2	CSA-RDRTGNGY-TF		3	
CC	8 / 11	8-3	20	CAV-GASRDYKL-SF	11-2	2-3	CAS-SFSSGTTDTQ-YF		3	
CD	25 / 2	25	42	CAY-GGSQGNL-IF	2	2-5	CAS-SQGDVAPGTQ-YF		3	
CE	5 / 20	5	40	CAE-VSGTYKY-IF	20-1	1-1	CSA-WDREVVGTEA-FF			37
CF	5 / 14	5	16	CAE-LGQKL-LF	14	2-5	CAS-SQSPGGTQ-YF			30
CG	5 / 29	5	37	CAE-STGKL-IF	29-1	1-4	CSV-GTGGTNEKL-FF			22
CH	5 / 20	5	31	CAE-DNNARL-MF	20-1	1-3	CSA-RIGVGNTI-YF			4
CI	8 / 9	8-3	39	CAD-PIEDAGNML-TF	9	2-2	CAS-SDGQLTAGEL-FF			4
CJ	29 / 4	29/DV5	34	CAA-TDNTDKL-IF	4-1	1-2	CAS-SRLGDY-TF			4
							Total # sequences	**32**	**31**	**27**

with mean frequencies of 2.2 ± 1.4 and 2.2 ± 1.2% of CD8$^+$ T cells, respectively (Fig. 5*b*, *panel ii*). Memory $NS3_{1073}$-specific CD8$^+$ T cell populations were detected at a higher frequency in donors with chronic HCV infection (13.0 ± 3.0%, Fig. 5, *c* and *d*). No discernable cross-reactive population was observed for either set of epitopes, of which only 0.19 ± 0.16 or 0.09 ± 0.08% of CD8$^+$ T cells in healthy donors were $M1_{58}$$^+$BMLF-1$^+$ or $NA_{231}$$^+$$NS3_{1073}$$^+$, respectively. Similarly, only 0.10 ± 0.14% of CD8$^+$ T cells were $NA_{231}$$^+$$NS3_{1073}$$^+$ in HCV-infected donors (Fig. 5*d*).

Lack of Heterologous Cross-reactivity after in Vitro Amplification—To determine whether the reported heterologous cross-reactivity could be a consequence of an *in vitro* amplification, epitope-specific CD8$^+$ T cell lines from healthy (Fig. 6) or HCV-infected donors (Fig. 7 and Table 4) were assessed for cross-reactivity by tetramer co-staining and an IFNγ$^+$ intracellular cytokine staining (ICS) assay. $M1_{58}$$^+$ and BMLF-1$^+$ CD8$^+$ T cell lines specifically responded to their cognate peptide, with 22.4 ± 16.8 and 17.9 ± 7.1% of the tetramer$^+$ CD8$^+$ T cells (Fig. 6, *a* and *b*) and 25.0 ± 12.3 and 9.7 ± 7.5% being IFNγ$^+$TNFα$^+$, respectively (Fig. 6, *c* and *d*). The frequency of CD8$^+$ T cells able to bind both tetramers and produce IFNγ$^+$TNFα$^+$ was just above background, showing the absence of CD8$^+$ T cells able to cross-react on both the $M1_{58}$ and BMLF-1 epitopes (Fig. 6).

Unlike previous studies (24), CD8$^+$ T cells did not expand in the presence of NA_{231}, and only 0.06 ± 0.04% and 0.19 ± 0.17% of CD8$^+$ T cells were NA_{231}-tetramer$^+$ or IFNγ$^+$TNFα$^+$ in an ICS assay, respectively (Fig. 7, *a* and *c*). Conversely, $NS3_{1073}$-specific CD8$^+$ T cells could be detected at 14.3 ± 11.7 and 4.0 ± 3.5% in the tetramer and ICS assays, respectively (Fig. 7, *b* and *d*). No cross-reactivity was detected in NA_{231} or $NS3_{1073}$-stimulated CD8$^+$ T cell lines either by tetramer co-staining (0.02 ± 0.01 and 0.09 ± 0.14% of CD8$^+$ T cells) (Fig. 7, *a* and *b*) or in the ICS assay (0.15 ± 0.11 and 0.60 ± 0.99% of CD8$^+$ T cells were IFNγ$^+$TNFα$^+$), respectively (Fig. 7, *c* and *d*). Together, these *ex vivo* and *in vitro* data highlight the lack of heterologous cross-reactivity toward $M1_{58}$ and BMLF-1 or NA_{231} and $NS3_{1073}$ epitopes, even following extended *in vitro* amplification.

No Cross-reactivity between Different NA_{231} Variant Peptides—Based on the low number of NA_{231} tetramer$^+$ CD8$^+$ T cells detected in our study, and because the NA protein is highly variable, we investigated whether the donors may have been exposed to other NA variants. We first examined the conservation of the NA_{231} peptide in the pH1N1, recent trivalent seasonal influenza vaccine strains, and Oceania-originated isolates (Table 5). A total of 28 variant peptides were identified. Mutations were common in the anchor P2 and P9 residues (buried residues; Fig. 1*c*), which are unlikely to affect TCR binding (Table 5). The P2 mutation, V2I, was common to the vaccine (71%) and Oceania (~67%) isolates and thus further increased the sequence homology to the $NS3_{1073}$ peptide. Three major variants from the NA_{231} WT CVNGSCFTV were identified and chosen for further analysis, namely C**I**NG**T**C**T**VV (P2-Ile-P5-Thro-P7-Thr-P8-Val), CVNGSCFTI (P9-Ile), and CI NGSCFTI (P2-Ile-P9-Ile) (Table 5).

To assess whether our HCV-infected donors had been exposed to a different NA_{231} variant (Table 5), CD8$^+$ T cell lines were established against each or a pool of the peptides containing WT NA_{231} and three NA_{231} variants, as well as WT $NS3_{1073}$ and a single $NS3_{1073}$ variant. No NA_{231}-specific CD8$^+$ T cells were expanded, despite extended *in vitro* amplification of up to 18 days (Fig. 8*a*). CD8$^+$ T cells were successfully expanded against the $NS3_{1073}$ peptides in both donors (Fig. 8*b*),

TABLE 3

$\alpha\beta$TCR usage for the recognition of NA_{231} and $NS3_{1073}$

Code represents the individual clonotypes. TRAV, variable α-chain gene usage; TRBV, β-chain gene usage; TRAJ, junction α-chain gene usage; TRBJ, junction β-chain gene usage; H, individual donor.

								Frequency							
								Naïve-NA_{231}			Naïve-$NS3_{1073}$			Memory-$NS3_{1073}$	
Code	Pairs	TRAV	TRAJ	CDR3α	TRBV	TRBJ	CDR3β	H-4	H-5	H-6	H-5	H-6	H-7	HCV-1	HCV-2
DA	35/29	35	52	CAG-QSNAGGTSYGKL-TF	29-1	2-7	CSV-EDGYEQ-YF	43							
DB	1/19	1-2	33	CAP-MDSNYQL-IW	19	2-6	CAS-SNSEGSGANVL-TF	14							
DC	6/14	6	38	CAL-PYNAGNNRKL-IW	14	2-7	CAS-SPLYVALREQ-YF	14							
DD	13/13	13-2	42	CAE-IHYGGSQGNL-IF	13	2-2	CAS-TSGNTGEL-FF	14							
DE	24/27	24	22	CAS-LSGSARQL-TF	27	2-1	CAS-SPTVAGEQ-FF	14							
DF	1/27	1-2	10	CAV-DILTGGGNKL-TF	27	1-5	CAS-NPLSAGNQPQ-HF		20						
DG	3/10	3	26	CAV-PGNYGQNF-VF	10-1	2-7	CAS-SEDQGLTATYEQ-YF		20						
DH	8/20	8-1	34	CAV-GSYNTDKL-IF	20-1	2-2	CSA-RVPDSNTGEL-FF		20						
DI	8/28	8-2	43	CAV-SDSYNDM-RF	28	1-2	CAS-SSPRTGYNYGY-TF		20						
DJ	13/6	13-1	39	CAE-NAGNML-TF	6	2-1	CAS-SPTSGGNNEQ-FF		20						
DK	4/23	4	32	CLV-GLYGGATNKL-IF	23-1	1-5	CAS-SQDRGVLVLIDQPQ-HF			25					
DL	8/1	8-6	34	CAV-SRSYNTDKL-IF	1-1	20-1	CSA-RTEGAEA-FF			25					
DM	12/2	12-2	24	CAV-NGDSWGKF-QF	2-5	14	CAS-SYWTGSSAETQ-YF			25					
DN	20/20	20	4	CAV-QAWFSGGYNKL-IF	20-1	2-1	CSA-RTSGDFGEQ-FF			25					
DO	4/4	4	39	CLV-GAGNML-TF	4	2-7	CAS-SQGGQGAPYEQ-YF				20				
DP	5/4	5	42	CAE-SGGSQGNL-IF	4-1	1-1	CAS-SQAENTEA-FF				20				
DQ	8/28	8-2	5	CAV-SSLMDTGRRAL-TF	28	2-2	CAS-SLLGLAGVGEL-FF				20				
DR	14/28	14	52	CAM-REDAGGTSYGKL-TF	28	2-1	CAS-SLTGTGFKQ-FF				20				
DS	26/28	26-2	52	CIL-RDLDGGTSYGKL-TF	28	2-3	CAS-SLTLAGGIGTDTQ-YF				20				
DT	4/7	4	36	CPF-QTGANNL-FF	7-2	2-7	CAS-SLGTGAPYEQ-YF					20			
DU	4/15	4	43	CLV-GAPGPGNTPL-VF	15	1-2	CAT-SNLDSFGGY-TF					20			
DV	4/17	4	43	CLV-GDNNNDM-RF	27	2-7	CAS-SLSTGAPYEQ-YF					20			
DW	38/11	38-2	45	CAY-RSPLSGGGADGL-TF	11-2	2-1	CAS-SLGPPPDNEQ-FF					20			
DX	38/19	38-2	40	CAY-TSGTYKY-IF	19	2-1	CAT-SPGQGFYNEQ-FF					20			
DY	4/28	4	9	CLK-AGGFKT-IF	28	2-7	CAS-RLLAGAYEQ-YF						33		
DZ	8/4	8-3	27	CAV-GAGTNAGKS-TF	4	1-1	CAS-SQESGTEAF-FG						33		
EA	22/18	22	47	CAV-ADPREYGNKL-VF	18	1-4	CAS-NRENEKL-FF						33		
EB	5/4	5	13	CAE-SGGYQKV-TF	4	1-1	CAS-SQEKGTEA-FF							38	
EC	4/2	4	28	CLV-GVPVGAGSYQL-TF	2	1-4	CAS-TTGSSEKL-FF							24	
ED	4/15	4	26	CLV-VGDNYGQNF-VF	15	1-2	CAT-STTFQTDYAEPYGY-TF							17	
EE	29/9	29	23	CAA-SARGNQGGKL-IF	9	2-2	CAS-SVDEGNTGEL-FF							7	
EF	38/28	38-2	45	CAY-RSATFSGGGADGL-TF	28	1-2	CAS-SRPVGLFNYGY-TF							7	
EG	4/4	4	9	CLV-GEGDTGGFKT-IF	4	1-2	CAS-SQVQTEPSGY-TF							3	
EH	4/16	4	45	CLV-GGGADGL-TF	16	2-7	CAS-SQEVTVPTYEQ-YF							3	
EI	4/4	4	43	CLD-SNDM-RF	4	2-7	CAS-SQAQSGTAPYEQ-YF								60
EJ	14/27	14	40	CAM-REFTSGTYKY-IF	27	2-5	CAS-SLTLGLAGVETQ-YF								27
EK	4/27	4	20	CLV-GSPNDYKL-SF	27	2-1	CAS-SSPSGRPTLYNEQ-FF								10
EL	38/15	38-2	17	CAY-SGIKAAGNKL-TF	15	1-5	CAT-SRDPQYQPQ-HF								3
							Total # of sequences	7	5	4	5	5	3	29	30

and CD8$^+$ T cells stimulated with the pool of peptides were able to respond only to both $NS3_{1073}$ peptides (Fig. 8*c*). Together, these data show that there is no cross-reactivity between WT and variants NA_{231} with $NS3_{1073}$ in donors with chronic HCV infection, in line with previously published data (26).

Discussion

Heterologous T cell cross-reactivity is a phenomenon whereby an individual CD8$^+$ T cell can recognize and respond to more than one viral antigen derived from unrelated viruses (41). It has the potential to be either beneficial, by increasing the chances that any given viral peptide is recognized by a CD8$^+$ T cell (28), or detrimental, by contributing to the CD8$^+$ T cell-mediated immunopathology associated with diseases such as EBV and HCV infection (23, 24). Because the few reports on T cell cross-reactivity in humans have shown conflicting results (20–25, 41), we investigated four epitopes from ubiquitous viruses (influenza, EBV, and HCV) restricted by the highly prevalent HLA-A*02:01 molecule. We aimed to elucidate the extent (if any) of the proposed heterologous cross-reactivity toward two distinct sets of HLA-A*02:01 restricted peptides: $M1_{58}$ (29) with BMLF-1 (27) and NA_{231} with $NS3_{1073}$ (27).

The most likely mechanism for heterologous T cell cross-reactivity would be that an individual CD8$^+$ T cell with a single TCR can recognize unrelated but similar pHLA complexes. This suggests that molecular mimicry would underpin heterologous T cell cross-reactivity, in a similar fashion to the interepitope cross-reactivity (5). Structures of the HLA-A*02:01 in complex with each paired peptide showed, however, that despite the sequence similarity of the paired peptides, the pHLA complexes display distinct architectures.

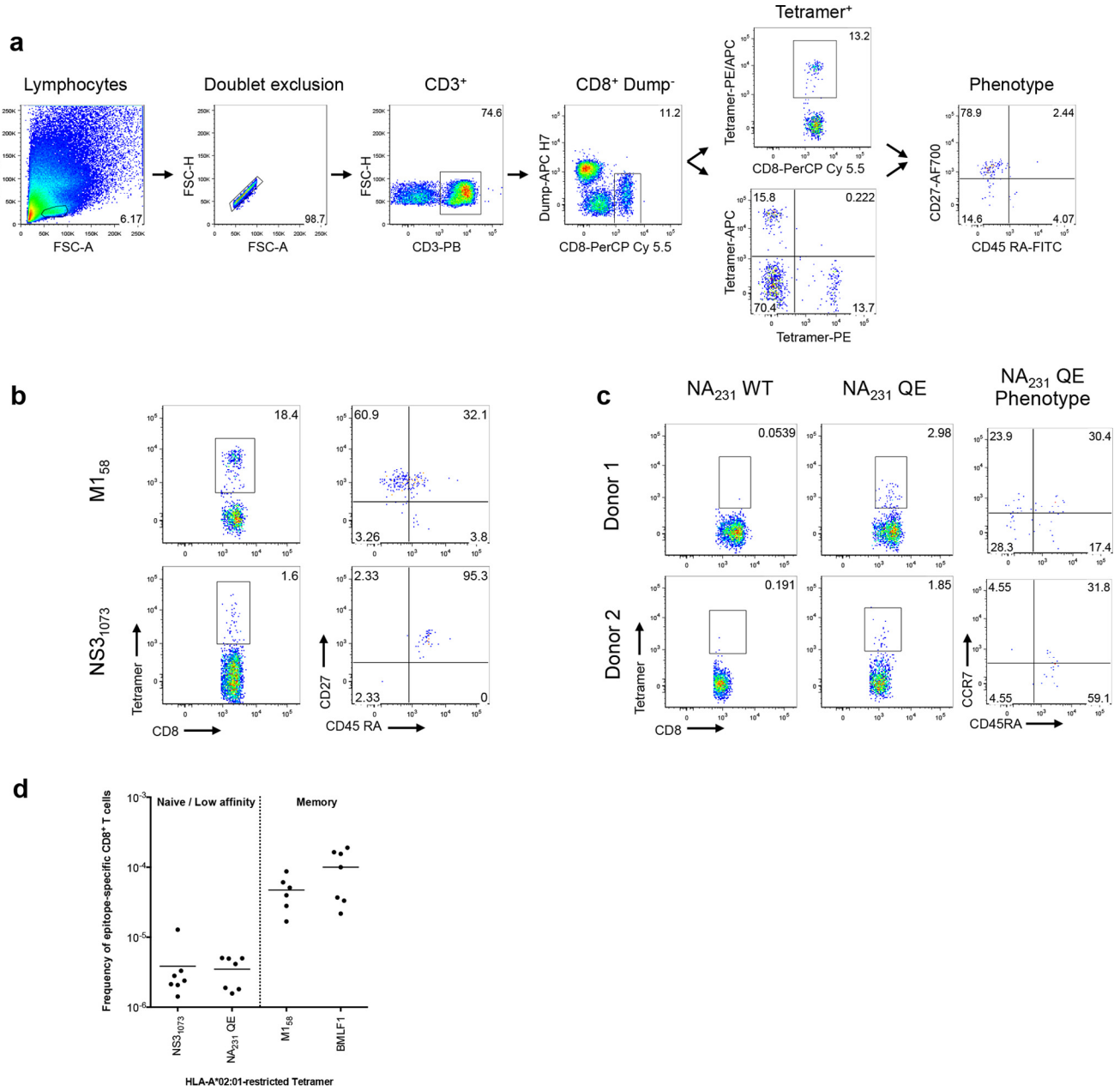

FIGURE 4. **Enumeration of naïve and memory HLA-*A*02:01*-restricted CD8⁺ T cell populations.** PBMCs from healthy HLA-*A*02:01*⁺ donors were tetramer-stained or co-stained with either $M1_{58}$ and BMLF-1 or NA_{231} and $NS3_{1073}$ conjugated to PE or APC. The samples were magnetically enriched and antibody-stained (as outlined under "Experimental Procedures") and gated on lymphocytes, singlets, $CD3^+$, $dump^-CD8^+$, and $tetramer^+$. *a*, representative dot plots describing the gating strategy used for data analysis of tetramer magnetic enrichment experiments. *b*, representative dot plots of naïve and memory tetramer positive populations and their respective phenotypes using αCD27 and αCD45 RA phenotypic markers. *c*, representative dot plots of PBMCs from two donors stained with either WT or HLA-*A*02:01*-QE mutant NA_{231}-specific tetramers and their phenotype using αCCR7 and αCD45 RA phenotypic markers. *d*, frequency of naïve, low affinity, and memory epitope-specific $CD8^+$ T cell populations in healthy HLA-*A*0201*⁺ donors after magnetic enrichment.

The $M1_{58}$ and BMLF-1 peptides share 56% sequence homology, and the conserved P6-Val adopts a different conformation between the two peptides. In BMLF-1, the P6-Val is solvent-exposed and available for TCR contact, whereas it is buried within the HLA-binding cleft in the $M1_{58}$ structure (29). This solvent-exposed P6-Val is important in the recognition of the BMLF-1 pHLA complex, as demonstrated by the structure of a prototypical public TCR (AS01) in complex with HLA-A*02:01-BMLF-1 (37). The highly conserved CDR3β loop positions itself atop the P6-Val, and the R*XXX*GN motif directly interacts with the P6-Val (36). The BMLF-1 peptide does not undergo structural change upon AS01 TCR binding, and moreover, alanine substitution of the P6-Val dramatically decreased the TCR affinity by 13-fold (37). Therefore, the buried conformation of P6-Val in the $M1_{58}$ complex would prevent binding by BMLF-1-specific $CD8^+$ T cells. From the structure of a conserved prototypical $TRBV19^+$ TCR (JM22) in complex with HLA-A*02:01-$M1_{58}$, it was observed that the $M1_{58}$ also does not undergo structural change upon TCR binding. Therefore, the solvent-exposed P6-Val of the BMLF-1 pHLA complex would cause steric clashes with the JM22 CDR3β loop, thus preventing binding (29, 30).

TABLE 4
Donors used in this study
H, healthy donor; HCV, HCV-infected donor.

			Figure										
	HLA-A	HLA-B	2A	2B	2C	4D	5Bi	5Bii	5D	6A-B	6C-D	7	8
H-1	0201, 1101	3501, 3901	Y								Y		
H-2	02:01, 11:01	35:03, 44:02	Y								Y		
H-3	02:01, 03:02	18:01, 35:08	Y								Y		
H-4	02:01, 2501	0702, 1801		Y		Y	Y	Y					
H-5	02, 24	07, 40		Y		Y		Y		Y	Y		
H-6	02,02	18,18		Y		Y	Y	Y					
H-7	02, 25	18, 44		Y									
H-8	02:01, 68:01	15:01, 40:01				Y							
H-9	02, 02	18, 27				Y							
H-10	0201, 0201	1501, 1801				Y	Y	Y					
H-11	0201, 2402	1302, 4403				Y	Y	Y					
H-12	0201, 0301	1401, 4002				Y	Y						
H-13	0101, 0201	0801, 4402								Y	Y		
H-14	0201, 0301	1402, 5801								Y	Y		
HCV-1	02:01, 03:01	08:01, 40:23			Y							Y	
HCV-2	02:01, 03	38:01, 45:01			Y							Y	Y
HCV-3	01:01, 02:01	35:02, 44:02							Y				
HCV-4	02:01, 31	18:01, 40							Y				
HCV-5	02:01, 32:01	15:01, 41:01										Y	Y
	Total # of donors		3	4	2	8	5	5	2	3	6	3	2

With regards to the NA_{231} and $NS3_{1073}$ peptide pair, although they have higher sequence homology (88%), they show opposing conformations for their conserved P6-Cys and P7-Phe/Trp residues. The NA_{231} P6-Cys is accessible for TCR binding, whereas the P7-Phe is buried. Conversely, the $NS3_{1073}$ P6-Cys is buried, and the P7-Trp is solvent-exposed. These changes completely alter the peptide conformation presented by HLA-A*02:01 to CD8$^+$ T cells for recognition.

Given the structural differences in the pHLA landscapes, the $\alpha\beta$TCR repertoire being utilized for the recognition of these peptides was also distinct. Paired analysis from three donors showed that no common TRAV/TRBV clonotype pairs were utilized to recognize either $M1_{58}$ or BMLF-1. The $M1_{58}$ $\alpha\beta$TCR repertoire has a distinct TRBV19 bias, as previously reported (20, 30, 31), whereas the BMLF-1 $\alpha\beta$TCR repertoire has a TRAV5 bias, which tends to pair with TRBV20–1 (37). Furthermore, the $\alpha\beta$TCR repertoire for recognition of NA_{231} and $NS3_{1073}$ was completely unrelated. Together, these data

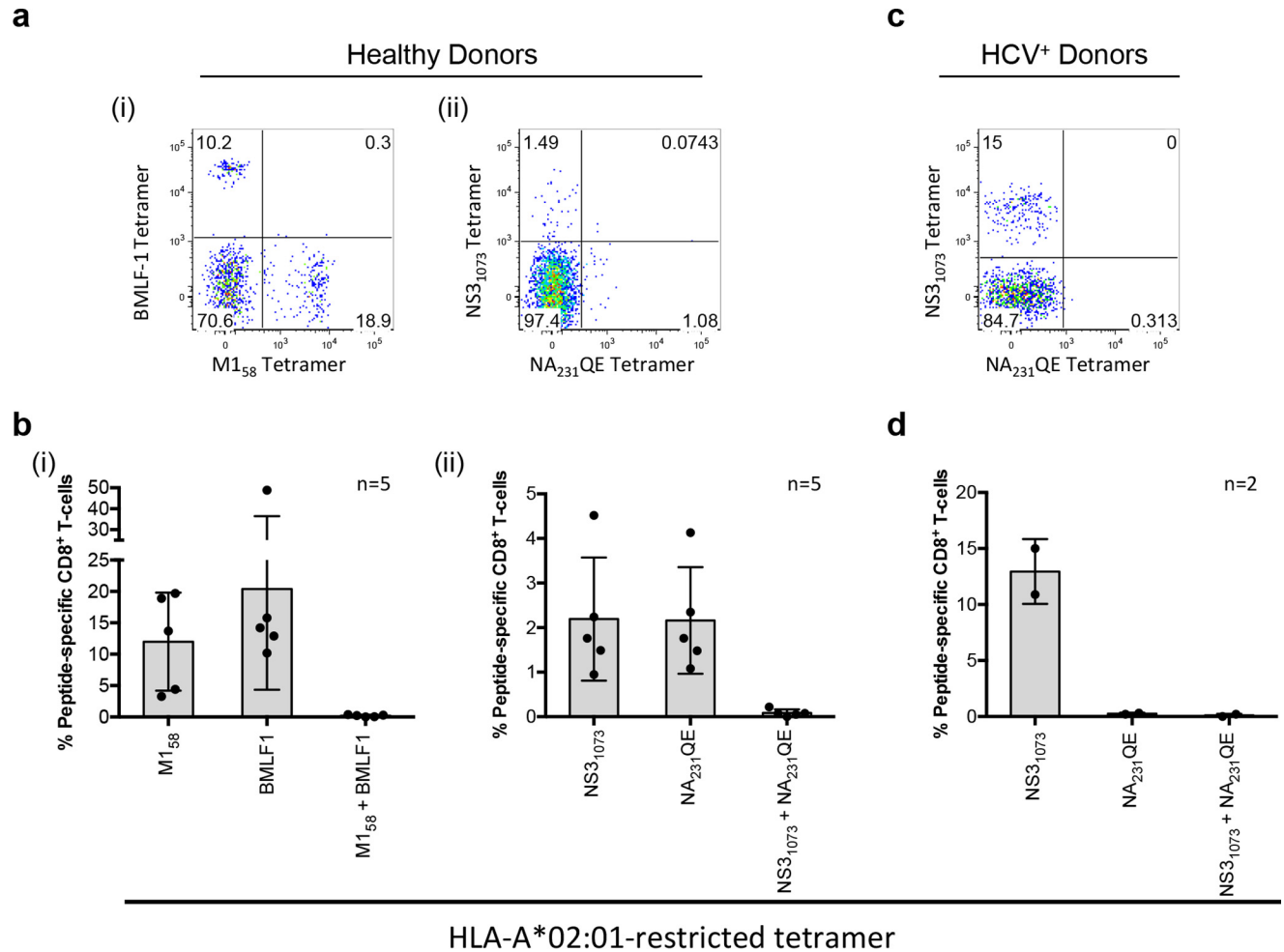

FIGURE 5. **Lack of heterologous T cell cross-reactivity between influenza-M1$_{58}$ and EBV-BMLF-1 or influenza-NA$_{231}$ and HCV-NS3$_{1073}$ detected directly *ex vivo*.** PBMCs from healthy and HCV-positive HLA-*A*02:01*$^+$ donors were tetramer co-stained with either $M1_{58}$ and BMLF-1 or $NS3_{1073}$ and NA_{231}QE tetramers. Following magnetic enrichment, PBMCs were surface-stained (as described under "Experimental Procedures") and gated on lymphocytes, singlets, CD3$^+$, and dump$^-$CD8$^+$. *a* and *b*, representative dot plots (*a*) and summary (*b*) of (*panel i*) memory $M1_{58}^+$ and BMLF-1$^+$ or (*panel ii*) low affinity NA_{231}^+ and naïve $NS3_{1073}^+$ tetramer$^+$ CD8$^+$ T cells derived from healthy donors ($n = 5$). The *bar charts* represent the means with the *error bars* representing standard deviation. *c* and *d*, representative dot plot (*c*) and summary (*d*) of low affinity NA_{231}^+ and memory $NS3_{1073}^+$-specific tetramer$^+$ CD8$^+$ T cells found in donors with chronic HCV infection ($n = 2$). The *bar charts* represent the means with the *error bars* representing standard deviation.

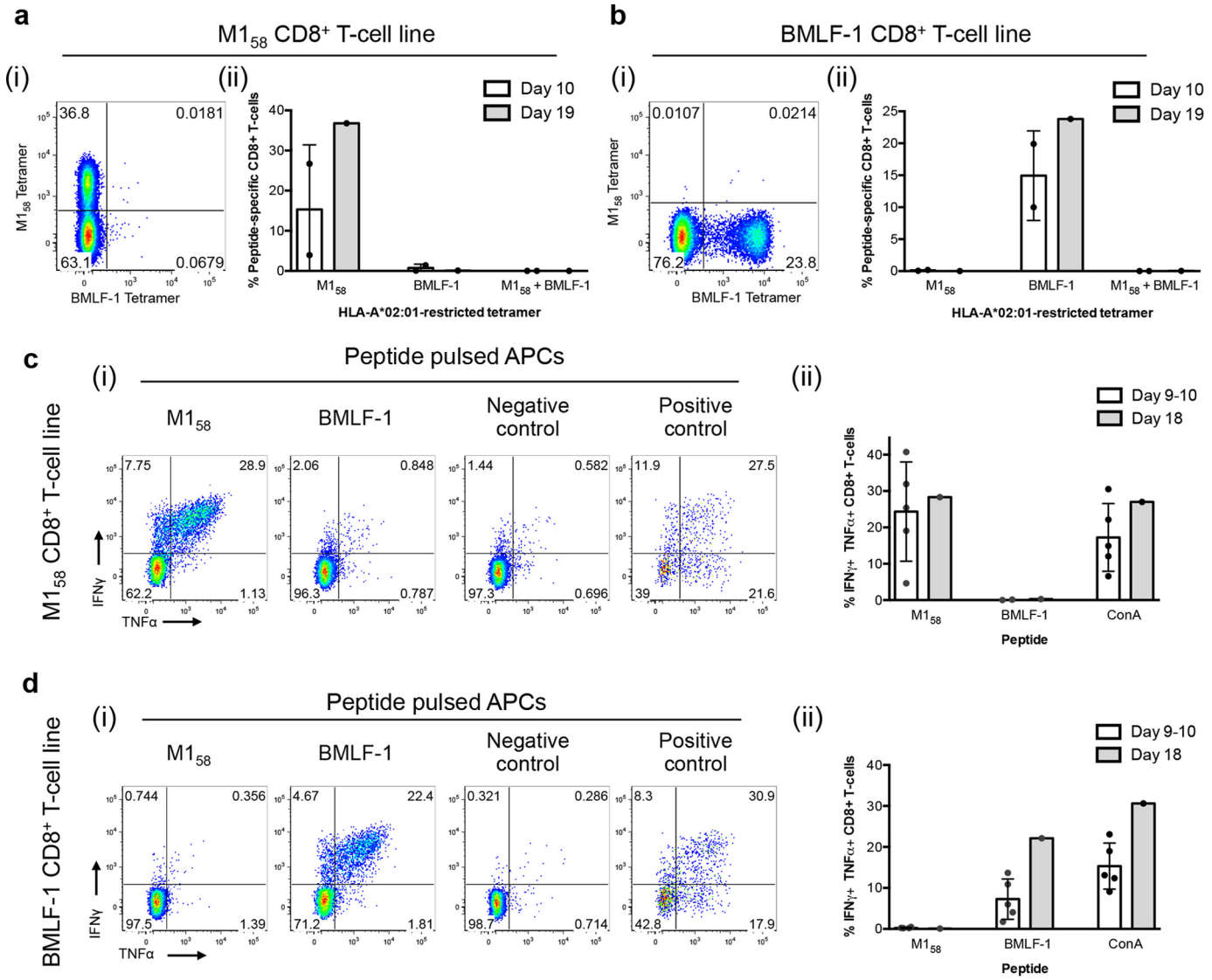

FIGURE 6. **Lack of heterologous T cell cross-reactivity was observed following *in vitro* culture of PBMCs with either the M1$_{58}$ or BMLF-1 peptides.** M1$_{58}$ and BMLF-1-specific CD8$^+$ T cell lines (stimulated for 9–19 days) from healthy donors were assessed for heterologous cross-reactivity by tetramer co-staining (with PE and APC) and an IFNγ^+TNFα^+ ICS assay. All CD8$^+$ T cell lines were antibody-stained (as described under "Experimental Procedures"), and the samples were gated on lymphocytes, singlets, CD3$^{mid\text{-}high}$, and CD8$^+$ T cells. *a*, representative dot plot (donor H-13) (*panel i*) and summary (*panel ii*) of epitope-specific tetramer$^+$ CD8$^+$ T cells in M1$_{58}$-specific CD8$^+$ T cell lines ($n = 3$). *b*, representative dot plot (donor H-13) (*panel i*) and summary (*panel ii*) of epitope-specific tetramer$^+$ CD8$^+$ T cells found in BMLF-1$_{280}$-specific CD8$^+$ T cell lines ($n = 3$). *c*, representative dot plots (donor H-13) (*panel i*) and summary (*panel ii*) of IFNγ^+TNFα^+ production (no-peptide control subtracted) derived from M1$_{58}$-specific CD8$^+$ T cell lines (APCs; $n = 6$) in response to each peptide and controls. *d*, representative dot plots (donor H-13) (*panel i*) and summary (*panel ii*) of IFNγ^+TNFα^+ production (no-peptide control subtracted) made by BMLF-1-specific CD8$^+$ T cell lines (APCs; $n = 6$) in response to each peptide and controls. The *bar charts* represent the means with the *error bars* representing standard deviation.

highlight that the paired peptides are presented differently by HLA-A*02:01 and consequently elicit very different $\alpha\beta$TCR repertoires. Thus, it is unlikely that heterologous T cell cross-reactivity could be occurring at a high frequency in HLA-A*02:01-positive donors between those two peptide pairs.

Using a combination of *ex vivo* and *in vitro* techniques, including high sensitivity tetramer magnetic enrichment, we were unable to detect any heterologous memory CD8$^+$ T cell cross-reactivity in healthy ($n = 12$) or HCV-infected ($n = 5$) donors. The prominent M1$_{58}$ and BMLF-1 CD8$^+$ T cell subsets were identified in all donors directly *ex vivo* and expanded to high levels following *in vitro* amplification. Despite this, no heterologous T cell cross-reactivity was detected even following extensive *in vitro* amplification. In addition, because the NA protein is variable between influenza strains, we tested a panel of common NA$_{231}$ variants in HCV-infected donors for heterologous T cell cross-reactivity with the NS3$_{1073}$ peptide. However, no responses were detected against the WT and variant NA$_{231}$ peptides. Together, these data imply that heterologous T cell cross-reactivity is not occurring frequently toward these epitopes in both healthy and HCV-infected donors.

The precise reasons for the conflicting reports on human heterologous T cell cross-reactivity are unknown. However, differences in methodology of T cell culture, donor cohorts, directionality, and strain specificity of the viral infection might influence the results. In our study, we have chosen to avoid prolonged stimulation of CD8$^+$ T cells or exposure to high concentration of numerous cytokines, to reproduce as closely

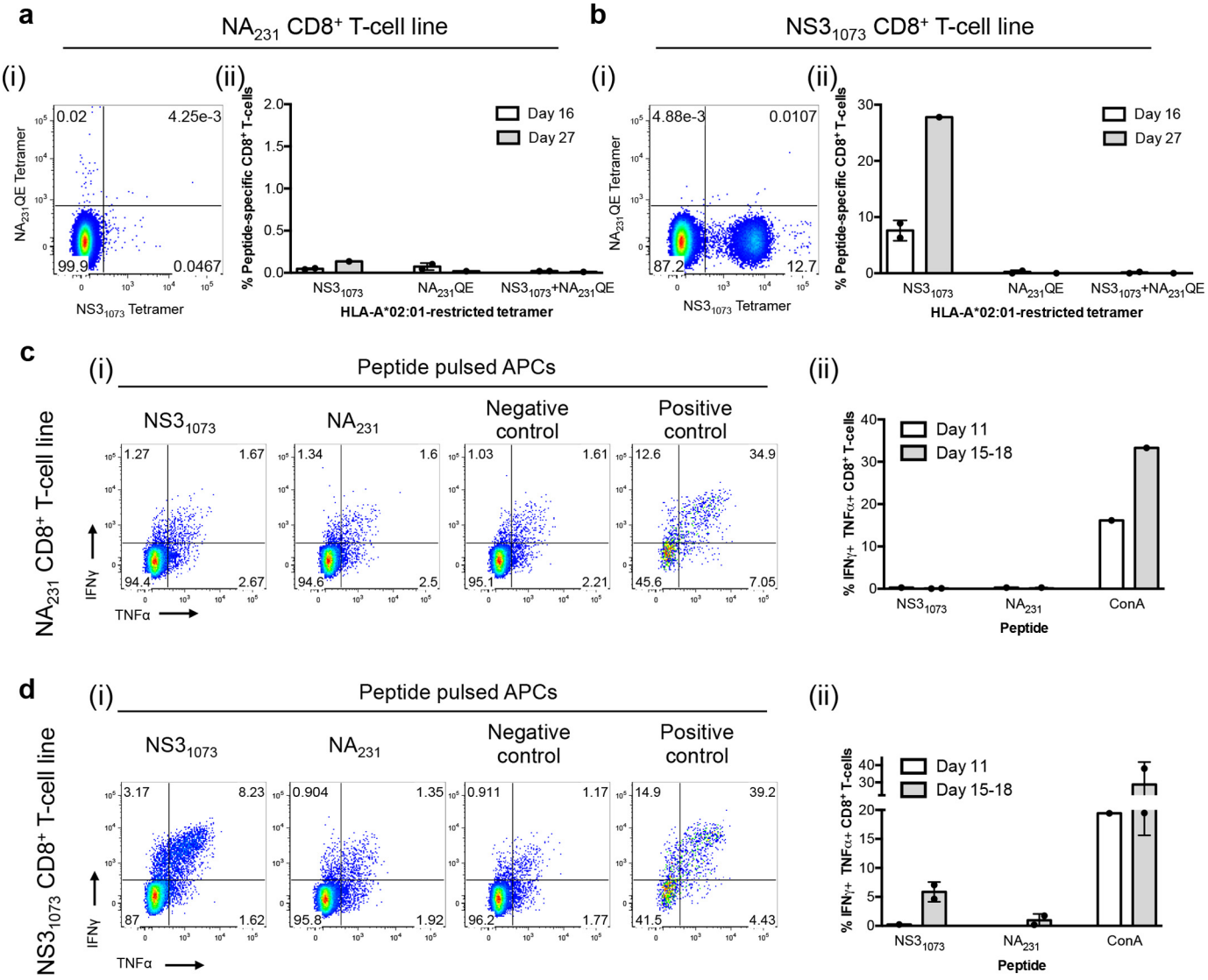

FIGURE 7. **Lack of heterologous T cell cross-reactivity following *in vitro* culture of PBMCs from donors with chronic HCV infection stimulated with either $NS3_{1073}$ or NA_{231} peptides.** PBMCs from HCV-infected individuals were stimulated (for 11–27 days) with NA_{231} or $NS3_{1073}$ peptides, and heterologous cross-reactivity was evaluated by tetramer co-staining and an IFNγ^+TNFα^+ ICS assay. The samples were stained (as described under "Experimental Procedures") and gated on lymphocytes, singlets, $CD3^{mid\text{-}high}$, and $CD8^+$ T cells. *a*, representative dot plot (donor HCV-2) (*panel i*) and summary (*panel ii*) of epitope-specific tetramer$^+$ $CD8^+$ T cells found in NA_{231}-stimulated $CD8^+$ T cell lines ($n = 3$). *b*, representative dot plot (donor HCV-2) (*panel i*) and summary (*panel ii*) of epitope-specific tetramer$^+$ $CD8^+$ T cells found in $NS3_{1073}$-specific $CD8^+$ T cell lines ($n = 3$). *c*, representative dot plots (donor HCV-2) (*panel i*) and summary (*panel ii*) of IFNγ^+TNFα^+ production (no-peptide control subtracted) made by NA_{231}-stimulated $CD8^+$ T cell lines (APCs; $n = 3$) in response to each peptide and controls. *d*, representative dot plots (donor HCV-2) (*panel i*) and summary (*panel ii*) of IFNγ^+TNFα^+ production (no-peptide control subtracted) derived from $NS3_{1073}$-specific $CD8^+$ T cell lines (APCs; $n = 3$) in response to each peptide and controls. The *bar charts* represent the means with the *error bars* representing standard deviation.

as possible a physiological $CD8^+$ T cell response. If heterologous T cell cross-reactivity occurs only in extreme circumstances of prolonged and potent T cell stimulation *in vitro*, it is therefore unlikely to happen frequently *in vivo* in humans. As shown in the present study, $NS3_{1073}$-specific $CD8^+$ T cells were frequent in HCV^+ donors but rare in healthy donors and with a naïve phenotype, and no cross-reactivity with NA_{231} was observed. Conversely, Urbani *et al.* (22) were able to detect T cell cross-reactivity for the $NA_{231}/NS3_{1073}$ pair, but only in a few HCV^+ donors with severe liver pathology. The directionality of viral infection, viral strains, and acute infection could thus impact on the presence or absence of heterologous $CD8^+$ T cell cross-reactivity.

Our data fit within the current published literature (22, 25, 26) and the lack of heterologous $CD8^+$ T cell cross-reactivity observed between the HLA-A*02:01-restricted epitopes ($M1_{58}$ with BMLF-1 and NA_{231} with $NS3_{1073}$) highlights that sequence similarity does not translate to structural mimicry and therefore does not lead to T cell cross-reactivity. In addition, limited sequence homology can lead to molecular mimicry, whereby different pMHC complexes can share structural features that will in turn be recognized by cross-reactive T cells (17, 42). Our data also fit with a recent study showing that TCRs are cross-reactive because of their "tolerance" to peptide changes (substitution with a similar residue or at a position not involved with TCR contact), leading to an overall molecular conservation (14). In conclusion, $CD8^+$ T cells can display a high level of specificity for their pHLA complex because of their $\alpha\beta$TCR, ensuring that autoimmunity is still a rare event within the population.

TABLE 5

NA_{231} sequences found in human influenza viruses isolated from 1935 to 2014

Sequences for conservation analysis were obtained from the NCBI Influenza Research Database. Full- length sequences were obtained and were aligned using the IEDB Analysis Resource. All vaccine strains, sequences from viruses isolated within Oceania, and all pH1N1 sequences were chosen for analysis. The frequency of each variant is shown in the table; the underlined residues are those that vary from the WT NA_{231} epitope.

		Frequency		
Sequence	Mutant	Vaccine	Oceania	pH1N1
CVNGSCFTV	WT	4	11	51
CINGTCTVV	V2I + S5T + F7T + T8V	71	63	
CVNGSCFTI	V9I	21	20	47
CMNGSCFTI	V2M + V9I	4	3	>1
CINGSCFTI	V2I + V9I		>1	>1
CINGTCAVV	V2I + S5T + F7A + T8V		2	
CINRTCTVV	V2I + G4R + S5T + F7T + T8V		>1	
CIYGTCTVV	V2I + N3Y + S5T + F7T + T8V		>1	
CVNGSCFTL	V9L			>1
CINGSCFTV	V2I			>1
CVNGSCFII	T8I + V9I			>1
CLNGSCFTV	V2L			>1
CVNGSCFIV	T8I			>1
CVNGSCFTM	V9M			>1
CANGSCFTV	V2A			>1
CVDGSCFTV	N3D			>1
CVHGSCFTV	N3H			>1
CVKGSCFTV	N3K			>1
CVNGACFTV	S5A			>1
CVNGFCFTV	S5F			>1
CVNGSYFTV	C6Y			>1
CVNGSCFAV	T8V			>1
CVNGSCFTT	V9T			>1
CANGSCFTI	V2A + V9I			>1
CVDGSCFTI	N3D + V9I			>1
CVNGFCFTI	S5F + V9I			>1
CVNGPCFTI	S5P + V9I			>1
CLNGSCFTI	V2L + V9I			>1
	Total # of sequences	*28*	*376*	*2430*
	Total strain coverage	*96%*	*95%*	*98%*

Experimental Procedures

Protein Purification, Crystallization, and Structure Determination—Soluble HLA-A*02:01 containing the $M1_{58}$, BMLF-1, NA_{231}, or $NS3_{1073}$ peptides were prepared as described previously (43, 44). Crystals of the HLA-A*02:01 in complex with the NA_{231} peptide were grown by the hanging drop, vapor diffusion method at 20 °C with a protein/reservoir drop ratio of 1:1, at a concentration of 10 mg/ml in 10 mM Tris-HCl, pH 8, 150 mM NaCl using 20% PEG 6K, 0.2 M NaCl, 0.1 M sodium citrate, pH 6.5. Prior to being flash frozen in liquid nitrogen, the crystals were soaked in a cryoprotectant solution containing mother liquor solution with 30% (w/v) PEG. The data were collected at the Australian Synchrotron (Clayton, Australia) on the 3BM1 Beamline (ADSC-Quantum 210 CCD detector) (45), processed with XDS software (46), and scaled using XSCALE software (46). The molecular replacement was performed with the PHASER program (47) using a previously solved HLA-A*02:01 peptide structure as the search model (PDB code 3GSO (43)). Manual model building was conducted using the Coot software (48) followed by maximum-likelihood refinement with the PHENIX program (49). The final HLA-A*02:01-NA_{231} model has been validated using the Protein Data Base validation web site (Table 1), and the coordinates have been submitted under the PDB code 5SWQ. All molecular graphics representations were created using PyMOL (50). Peptide sequence alignment was performed using the Clustalw server, and the sequence homology encompasses identical and chemically similar residues.

Thermal Stability Assay—To assess the stability of each peptide within the HLA-A*02:01 molecule, a thermal shift assay was performed as previously described (30).

Human Samples—Buffy packs from healthy blood donors (seronegative for HIV, HBV, and HCV) were obtained from the Australian Red Cross Blood Service (West Melbourne, Australia). Blood from HCV-infected subjects was collected as a part of social network study of intravenous drug users (Burnet Institute, Melbourne, Australia (51). HCV status was assessed via serology and the presence of viral RNA at the Victorian Infectious Diseases Reference Laboratory (Parkville, Australia). Samples were HLA-typed by the Victorian Transplant and Immunogenetics Service (West Melbourne, Australia) at the Australian Red Cross Blood Service tissue-typing laboratory. HLA-A*02:01-positive, HBV-negative, HIV-negative injected-drug users were selected. Donors used in this study are listed in Table 4. The experiments conformed to the NHMRC Code of Practice and were approved by the University of Melbourne Research Human Ethics Committee.

Separation of PBMCs from Whole Blood—PBMCs were separated from peripheral blood by density gradient centrifugation over Ficoll-Paque Plus (Sigma-Aldrich). Diluted blood was layered onto 15 ml of Ficoll-Paque Plus and centrifuged. PBMCs were collected from the interface of the Ficoll, washed three times, resuspended in freezing medium (10% dimethyl sulfoxide; Sigma-Aldrich) in heat-inactivated FCS (Bovogen Biological, Keilor East, Australia), and stored in liquid nitrogen.

Peptides and Tetramers—The following HLA-A*02:01-restricted peptides were purchased from Genscript: HCV-$NS3_{1073-1081}$ and variant peptides (CINGVCWTV; C**V**NGVC-WTV), influenza-$NA_{231-239}$ WT and variant peptides (CVNGSCFTV; CVNGSCFT**I**; C**I**NGSCFT**I**; C**I**NG**T**C**TV**V), influenza-$M1_{58-66}$ (GILGFVFTL), and BMLF-1 (GLCTL-VAML). Wild type HLA-A*02:01 and CD8β-binding HLA-A*02:01 mutant (Q115E; QE) (40) monomers were purchased from the Immuno ID Facility (Department of Microbiology and Immunology, University of Melbourne, Melbourne, Australia).

CD8$^+$ T Cell Lines—PBMCs were thawed, washed, and rested for 1 h in RF10 (RPMI (Gibco) supplemented with 10–20% FCS, 5 mM HEPES (MP Biomedicals), 100 μg/ml streptomycin (Gibco), 100 units/ml benzylpenicillin (CSL, Parkville, Australia), 2 mM L-glutamine (MP Biomedicals), 55 μM β-mercaptoethanol (Sigma-Aldrich), and 100 mM non-essential amino acids (Gibco)). Samples were split into stimulators and responders at a ratio of 1:2 for healthy donors or 1:1 for HCV-infected individuals. Stimulators were pulsed with 10 μg/ml peptide for 90 min, washed, and added to the responders. Media half changes were done twice weekly with RF10 supplemented with 10–20 units/ml of IL-2 with or without 50% T cell growth factor (supernatant from MLA44 cell). Cultures derived from HCV-infected individuals were supplemented with 25 units/ml IL-7 on day 3. The cultures were restimulated on day 7 and then weekly for CD8$^+$ T cell lines at a 1:10–15 stimulators to responders ratio with C1R-HLA-A*02:01-expressing cells pulsed with 10 μg/ml peptide for 60 min and gamma-irradiated at 8,000 rad.

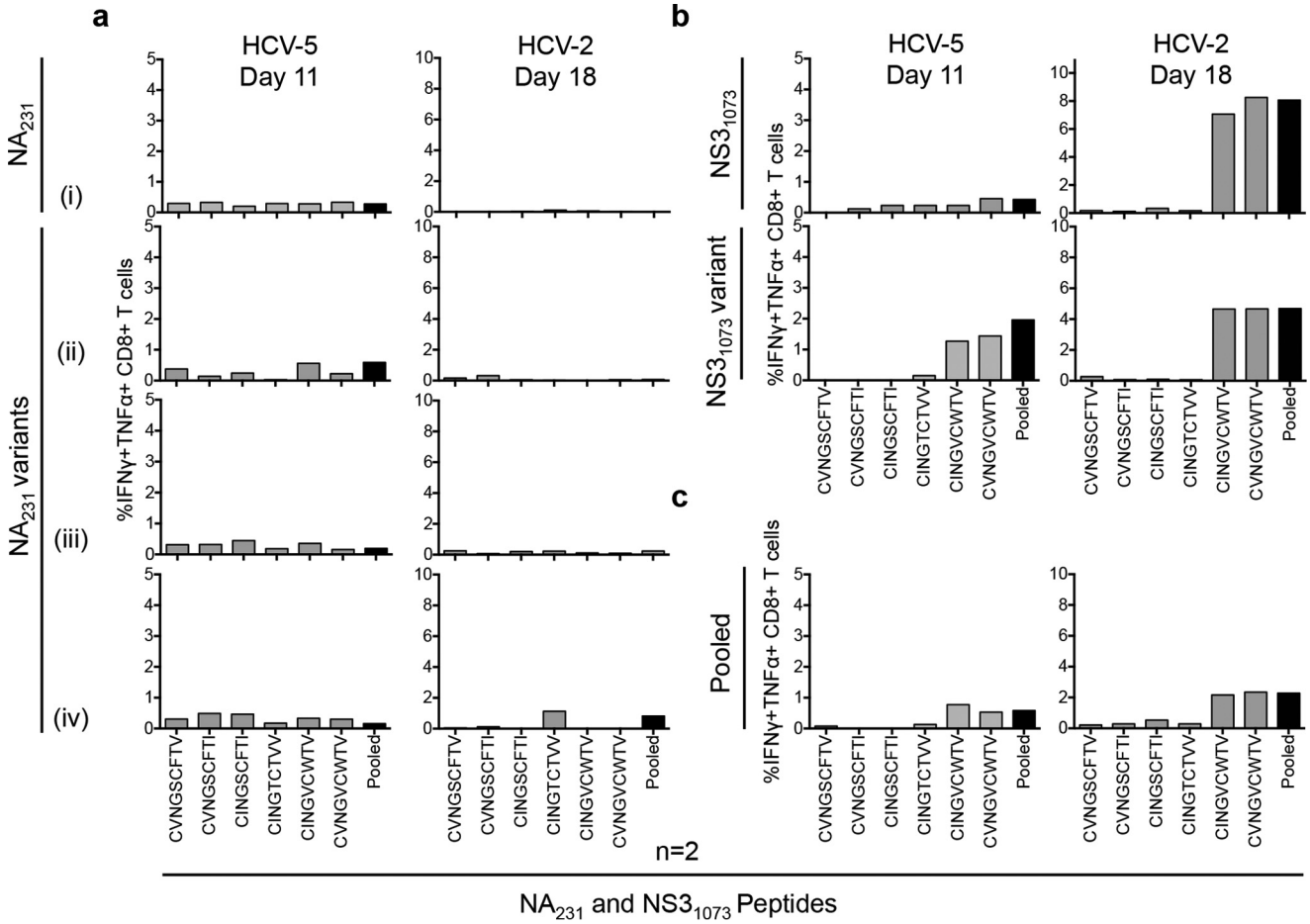

FIGURE 8. **PBMCs from individuals chronically infected with HCV do not expand to NA_{231} variant peptides *in vitro*.** CD8$^+$ T cell lines from donors with chronic HCV infection were raised against WT and variant NA_{231} peptides, and WT or variant $NS3_{1073}$ peptides, or a pool of all peptides for 11–18 days ($n = 2$). CD8$^+$ T cell responses toward each individual peptide were assessed in an IFNγ^+TNFα^+ ICS assay. The cells were stained (as described under "Experimental Procedures") and gated on lymphocytes, singlets, CD3$^{mid\text{-}high}$, and CD8$^+$ T cells. *a*, proportion of IFNγ^+TNFα^+ production (no peptide control subtracted) by CD8$^+$ T cells lines raised against NA_{231}-WT (CVNGSCFTV) (*panel i*), NA_{231}-I9 CVNGSCFT**I** (*panel ii*), NA_{231}-I2-I9 (C**I**NGSCFT**I**) (*panel iii*), and NA_{231}-I2-T5-T7-V8 (C**I**NG**T**C**T**V**V**) (*panel iv*) in response to each peptide. *b*, proportion of IFNγ^+TNFα^+ production toward each peptide (no peptide control subtracted) by CD8$^+$ T cells lines raised against WT $NS3_{1073}$ (CINGVGWTV) and $NS3_{1073}$-V2 (CVNGVGWTV). *c*, proportion of IFNγ^+TNFα^+ production (no peptide control subtracted) by CD8$^+$ T cells raised against pooled peptides, in response to each peptide.

Intracellular Cytokine Staining—CD8$^+$ T cell lines were stimulated with C1R-HLA-A*02:01-expressing cells pulsed with 10 μg/ml of peptide for 1 h at a ratio of 1:2 stimulators to responders in the presence of IL-2. The cells were incubated for 1 h and then supplemented with 10 μg/ml brefeldin A (Sigma-Aldrich) and incubated for a further 5 h. Cells were then surface-stained with αCD3-PeCy7 and αCD8-PerCP (BD Biosciences) for 30 min and fixed in 1% paraformaldehyde (PFA; Electron Microscopy Sciences, Hatfield, PA) for 15 min. The cells were permeabilized with 0.3% saponin (Sigma) diluted in PBS and stained for internal cytokines αIFNγ (PE or FITC) and αTNFα (FITC or PE) overnight (BD Biosciences). The samples were acquired on the BD FACS Canto II (BD Biosciences) and analyzed using Flowjo software (Treestar).

Tetramer Staining—CD8$^+$ T cell lines were stained with tetramers for 1 h at room temperature. The cells were subsequently surface-stained with αCD3-PeCy7, αCD8-PerCP/PerCPCy5.5, αCD27-APCH7, and αCD45RA-FITC (BD Biosciences) in PBS for 30 min, fixed in 1% PFA, acquired on the BD FACS Canto II, and analyzed using Flowjo software. The markers CD27, CCR7, and CD45RA were utilized to determine the phenotype of epitope-specific cells. Naïve cells are CD27$^+$ or CCR7$^+$CD45RA$^+$, whereas cells of all other combinations represent memory CD8$^+$ T cells.

Magnetic Enrichment of Peptide-specific CD8$^+$ T Cells ex Vivo—PBMCs were incubated in 20 μl/1 $\times$ 10^7 cells FcR block (Miltenyi Biotech) for 15 min after thawing. Tetramer staining of 1 $\times$ 10^7 cells (for memory CD8$^+$ T cells) or 5 $\times$ 10^7 cells (for naïve or low affinity CD8$^+$ T cells) was performed at a 1:100 dilution of PE- or APC-conjugated tetramers in sorter buffer (PBS, 0.5% BSA (Gibco), 2 mM EDTA (Ajax Finechem)) for 1 h. The cells were incubated with 100 μl of αPE and 100 μl of αAPC microbeads (Miltenyi Biotech) in 300 μl of sorter buffer for 30 min. The cells were thoroughly washed, positively enriched by running twice over a LS magnetic column (Miltenyi Biotech), and then surface-stained with αCD3-PB αCD8-PerCP Cy5.5, αCD4-APCH7, and αCD45RA-FITC in combination with αCD27-AF700, αCD14-APCH7, and αCD19-APCH7 or αCCR7-APC and αCD14-PeCy7 (BD Biosciences, CA, USA) for 30 min. The samples were fixed with 1% PFA, acquired on the BD FACS LSR II (BD Biosciences), and analyzed using Flowjo software.

Single-cell Sorting and Multiplex PCR—Epitope-specific CD8$^+$ T cells were antibody-stained, and CD3$^+$CD8$^+$-tetramer$^+$ cells were single-cell sorted directly into 96-well PCR plates (Eppendorf, Hamburg, Germany) using the BD FACS Aria II (BD Biosciences). cDNA was synthesized using the VILO RT kit (Invitrogen). Multiplex nested PCR was performed as previously described (34, 52). Briefly, the external round was performed with 40 Vα-external and 27 Vβ-external primers and the Cα-external and Cβ external primers. The internal PCR rounds were performed individually with the 40 Vα-internal and Cα-internal or the 27 Vβ-internal and the Cβ-internal primers (34, 52). PCR products were detected on a 2% agarose gel and purified using Exosap (Affymetrix) or Exostar (GE Healthcare). The sequencing reaction was performed using the C-internal primer and BigDyeV3.1 (Applied Biosystems) and cleaned on DyeEx sequencing plates (Qiagen). Sequencing was performed by the Pathology Department at the University of Melbourne (Melbourne, Australia). The sequences were analyzed using FinchTV, and V and J region usage was identified by IMGT query (53). CDR3 amino acid sequences described within the manuscript are productive (without stop codons and with an in-frame junction) $\alpha\beta$TCR pairs and start from CDR3 position 1, as determined by the IMGT software. CDR3 length and motifs are from position 4. Samples with two α or β chains were dissected by performing an internal round of PCR with the specific individual primers and then sequenced as above. Where possible, both chains were resolved; however, in a few instances only the dominant chain could be resolved. Samples with TRBV19 ($M1_{58}{}^+CD8^+$ T cell repertoire) had the internal round of PCR repeated with TRBV19 and were subsequently sequenced with the TRBV19 forward primer. IMGT nomenclature was used (54). CDR3 motif conservation analysis (Fig. 8) was generated using the Seq2Logo 2.0 server (55) using the Shannon logo type, no clustering, 0 weight on prior, and seq2logo default amino acid color settings.

Author Contributions—E. J. G., T. M. J., S. A. V., J. R., M. B., S. G., and K. K. designed the research; E. J. G., T. M. J., S. A. V., S. G., and K. K. performed the research; M. H., M. B., L. W., and J. R. contributed new reagents/analytic tools; E. J. G., T. M. J., S. A. V., S. G., and K. K. analyzed the data; and E. J. G., T. M. J., J. R., S. G., and K. K. wrote the paper.

Acknowledgments—We thank staff at the Australian Synchrotron for technical assistance and Julia Archbold (Corrected Science Writing and Editing Services, Australia), who provided editorial support for this manuscript.

References

1. Chothia, C., Boswell, D. R., and Lesk, A. M. (1988) The outline structure of the T-cell $\alpha\beta$ receptor. *EMBO J.* **7,** 3745–3755
2. Rossjohn, J., Gras, S., Miles, J. J., Turner, S. J., Godfrey, D. I., and McCluskey, J. (2015) T cell antigen receptor recognition of antigen-presenting molecules. *Annu. Rev. Immunol.* **33,** 169–200
3. Jerne, N. K. (1955) The natural-selection theory of antibody formation. *Proc. Natl. Acad. Sci. U.S.A.* **41,** 849–857
4. Mason, D. (1998) A very high level of crossreactivity is an essential feature of the T-cell receptor. *Immunol. Today* **19,** 395–404
5. Valkenburg, S. A., Gras, S., Guillonneau, C., La Gruta, N. L., Thomas, P. G., Purcell, A. W., Rossjohn, J., Doherty, P. C., Turner, S. J., and Kedzierska, K. (2010) Protective efficacy of cross-reactive CD8+ T cells recognising mutant viral epitopes depends on peptide-MHC-I structural interactions and T cell activation threshold. *PLoS Pathogens* **6,** e1001039
6. Kedzierska, K., Guillonneau, C., Gras, S., Hatton, L. A., Webby, R., Purcell, A. W., Rossjohn, J., Doherty, P. C., and Turner, S. J. (2008) Complete modification of TCR specificity and repertoire selection does not perturb a CD8+ T cell immunodominance hierarchy. *Proc. Natl. Acad. Sci. U.S.A.* **105,** 19408–19413
7. Wooldridge, L., Ekeruche-Makinde, J., van den Berg, H. A., Skowera, A., Miles, J. J., Tan, M. P., Dolton, G., Clement, M., Llewellyn-Lacey, S., Price, D. A., Peakman, M., and Sewell, A. K. (2012) A single autoimmune T cell receptor recognizes more than a million different peptides. *J. Biol. Chem.* **287,** 1168–1177
8. Brehm, M. A., Pinto, A. K., Daniels, K. A., Schneck, J. P., Welsh, R. M., and Selin, L. K. (2002) T cell immunodominance and maintenance of memory regulated by unexpectedly cross-reactive pathogens. *Nat. Immunol.* **3,** 627–634
9. Chen, A. T., Cornberg, M., Gras, S., Guillonneau, C., Rossjohn, J., Trees, A., Emonet, S., de la Torre, J. C., Welsh, R. M., and Selin, L. K. (2012) Loss of anti-viral immunity by infection with a virus encoding a cross-reactive pathogenic epitope. *PLoS Pathogens* **8,** e1002633
10. Chen, H. D., Fraire, A. E., Joris, I., Brehm, M. A., Welsh, R. M., and Selin, L. K. (2001) Memory CD8+ T cells in heterologous antiviral immunity and immunopathology in the lung. *Nat. Immunol.* **2,** 1067–1076
11. Kim, S. K., Cornberg, M., Wang, X. Z., Chen, H. D., Selin, L. K., and Welsh, R. M. (2005) Private specificities of CD8 T cell responses control patterns of heterologous immunity. *J. Exp. Med.* **201,** 523–533
12. Selin, L. K., Varga, S. M., Wong, I. C., and Welsh, R. M. (1998) Protective heterologous antiviral immunity and enhanced immunopathogenesis mediated by memory T cell populations. *J. Exp. Med.* **188,** 1705–1715
13. Shen, Z. T., Nguyen, T. T., Daniels, K. A., Welsh, R. M., and Stern, L. J. (2013) Disparate epitopes mediating protective heterologous immunity to unrelated viruses share peptide-MHC structural features recognized by cross-reactive T cells. *J. Immunol.* **191,** 5139–5152
14. Birnbaum, M. E., Mendoza, J. L., Sethi, D. K., Dong, S., Glanville, J., Dobbins, J., Ozkan, E., Davis, M. M., Wucherpfennig, K. W., and Garcia, K. C. (2014) Deconstructing the peptide-MHC specificity of T cell recognition. *Cell* **157,** 1073–1087
15. Colf, L. A., Bankovich, A. J., Hanick, N. A., Bowerman, N. A., Jones, L. L., Kranz, D. M., and Garcia, K. C. (2007) How a single T cell receptor recognizes both self and foreign MHC. *Cell* **129,** 135–146
16. Garcia, K. C., Degano, M., Pease, L. R., Huang, M., Peterson, P. A., Teyton, L., and Wilson, I. A. (1998) Structural basis of plasticity in T cell receptor recognition of a self peptide-MHC antigen. *Science* **279,** 1166–1172
17. Macdonald, W. A., Chen, Z., Gras, S., Archbold, J. K., Tynan, F. E., Clements, C. S., Bharadwaj, M., Kjer-Nielsen, L., Saunders, P. M., Wilce, M. C., Crawford, F., Stadinsky, B., Jackson, D., Brooks, A. G., Purcell, A. W., *et al.* (2009) T cell allorecognition via molecular mimicry. *Immunity* **31,** 897–908
18. Yin, L., Huseby, E., Scott-Browne, J., Rubtsova, K., Pinilla, C., Crawford, F., Marrack, P., Dai, S., and Kappler, J. W. (2011) A single T cell receptor bound to major histocompatibility complex class I and class II glycoproteins reveals switchable TCR conformers. *Immunity* **35,** 23–33
19. Clute, S. C., Naumov, Y. N., Watkin, L. B., Aslan, N., Sullivan, J. L., Thorley-Lawson, D. A., Luzuriaga, K., Welsh, R. M., Puzone, R., Celada, F., and Selin, L. K. (2010) Broad cross-reactive TCR repertoires recognizing dissimilar Epstein-Barr and influenza A virus epitopes. *J. Immunol.* **185,** 6753–6764
20. Clute, S. C., Watkin, L. B., Cornberg, M., Naumov, Y. N., Sullivan, J. L., Luzuriaga, K., Welsh, R. M., and Selin, L. K. (2005) Cross-reactive influenza virus-specific CD8+ T cells contribute to lymphoproliferation in Epstein-Barr virus-associated infectious mononucleosis. *J. Clin. Invest.* **115,** 3602–3612
21. Odumade, O. A., Knight, J. A., Schmeling, D. O., Masopust, D., Balfour, H. H., Jr, and Hogquist, K. A. (2012) Primary Epstein-Barr virus infection does not erode preexisting CD8$^+$ T cell memory in humans. *J. Exp. Med.* **209,** 471–478

22. Urbani, S., Amadei, B., Fisicaro, P., Pilli, M., Missale, G., Bertoletti, A., and Ferrari, C. (2005) Heterologous T cell immunity in severe hepatitis C virus infection. *J. Exp. Med.* **201,** 675–680
23. Kasprowicz, V., Ward, S. M., Turner, A., Grammatikos, A., Nolan, B. E., Lewis-Ximenez, L., Sharp, C., Woodruff, J., Fleming, V. M., Sims, S., Walker, B. D., Sewell, A. K., Lauer, G. M., and Klenerman, P. (2008) Defining the directionality and quality of influenza virus-specific CD8+ T cell cross-reactivity in individuals infected with hepatitis C virus. *J. Clin. Invest.* **118,** 1143–1153
24. Wedemeyer, H., Mizukoshi, E., Davis, A. R., Bennink, J. R., and Rehermann, B. (2001) Cross-reactivity between hepatitis C virus and Influenza A virus determinant-specific cytotoxic T cells. *J. Virol.* **75,** 11392–11400
25. Neveu, B., Debeaupuis, E., Echasserieau, K., le Moullac-Vaidye, B., Gassin, M., Jegou, L., Decalf, J., Albert, M., Ferry, N., Gournay, J., Houssaint, E., Bonneville, M., and Saulquin, X. (2008) Selection of high-avidity CD8 T cells correlates with control of hepatitis C virus infection. *Hepatology* **48,** 713–722
26. Pasetto, A., Frelin, L., Brass, A., Yasmeen, A., Koh, S., Lohmann, V., Bartenschlager, R., Magalhaes, I., Maeurer, M., Sällberg, M., and Chen, M. (2012) Generation of T-cell receptors targeting a genetically stable and immunodominant cytotoxic T-lymphocyte epitope within hepatitis C virus non-structural protein 3. *J. Gen. Virol.* **93,** 247–258
27. Reiser, J. B., Legoux, F., Gras, S., Trudel, E., Chouquet, A., Léger, A., Le Gorrec, M., Machillot, P., Bonneville, M., Saulquin, X., and Housset, D. (2014) Analysis of relationships between peptide/MHC structural features and naive T cell frequency in humans. *J. Immunol.* **193,** 5816–5826
28. Selin, L. K., Brehm, M. A., Naumov, Y. N., Cornberg, M., Kim, S. K., Clute, S. C., and Welsh, R. M. (2006) Memory of mice and men: CD8+ T-cell cross-reactivity and heterologous immunity. *Immunol. Rev.* **211,** 164–181
29. Ishizuka, J., Stewart-Jones, G. B., van der Merwe, A., Bell, J. I., McMichael, A. J., and Jones, E. Y. (2008) The structural dynamics and energetics of an immunodominant T cell receptor are programmed by its Vβ domain. *Immunity* **28,** 171–182
30. Valkenburg, S. A., Josephs, T. M., Clemens, E. B., Grant, E. J., Nguyen, T. H., Wang, G. C., Price, D. A., Miller, A., Tong, S. Y., Thomas, P. G., Doherty, P. C., Rossjohn, J., Gras, S., and Kedzierska, K. (2016) Molecular basis for universal HLA-A*0201-restricted CD8+ T-cell immunity against influenza viruses. *Proc. Natl. Acad. Sci. U.S.A.* **113,** 4440–4445
31. Stewart-Jones, G. B., McMichael, A. J., Bell, J. I., Stuart, D. I., and Jones, E. Y. (2003) A structural basis for immunodominant human T cell receptor recognition. *Nat. Immunol.* **4,** 657–663
32. Liu, Y. C., Chen, Z., Neller, M. A., Miles, J. J., Purcell, A. W., McCluskey, J., Burrows, S. R., Rossjohn, J., and Gras, S. (2014) A molecular basis for the interplay between T cells, viral mutants, and human leukocyte antigen micropolymorphism. *J. Biol. Chem.* **289,** 16688–16698
33. Miles, J. J., Borg, N. A., Brennan, R. M., Tynan, F. E., Kjer-Nielsen, L., Silins, S. L., Bell, M. J., Burrows, J. M., McCluskey, J., Rossjohn, J., and Burrows, S. R. (2006) TCR α genes direct MHC restriction in the potent human T cell response to a class I-bound viral epitope. *J. Immunol.* **177,** 6804–6814
34. Nguyen, T. H., Rowntree, L. C., Pellicci, D. G., Bird, N. L., Handel, A., Kjer-Nielsen, L., Kedzierska, K., Kotsimbos, T. C., and Mifsud, N. A. (2014) Recognition of distinct cross-reactive virus-specific CD8+ T cells reveals a unique TCR signature in a clinical setting. *J. Immunol.* **192,** 5039–5049
35. Lehner, P. J., Wang, E. C., Moss, P. A., Williams, S., Platt, K., Friedman, S. M., Bell, J. I., and Borysiewicz, L. K. (1995) Human HLA-A0201-restricted cytotoxic T lymphocyte recognition of influenza A is dominated by T cells bearing the Vβ 17 gene segment. *J. Exp. Med.* **181,** 79–91
36. Moss, P. A., Moots, R. J., Rosenberg, W. M., Rowland-Jones, S. J., Bodmer, H. C., McMichael, A. J., and Bell, J. I. (1991) Extensive conservation of α and β chains of the human T-cell antigen receptor recognizing HLA-A2 and influenza A matrix peptide. *Proc. Natl. Acad. Sci. U.S.A.* **88,** 8987–8990
37. Miles, J. J., Bulek, A. M., Cole, D. K., Gostick, E., Schauenburg, A. J., Dolton, G., Venturi, V., Davenport, M. P., Tan, M. P., Burrows, S. R., Wooldridge, L., Price, D. A., Rizkallah, P. J., and Sewell, A. K. (2010) Genetic and structural basis for selection of a ubiquitous T cell receptor deployed in Epstein-Barr virus infection. *PLoS Pathogens* **6,** e1001198
38. Valkenburg, S. A., Gras, S., Guillonneau, C., Hatton, L. A., Bird, N. A., Twist, K. A., Halim, H., Jackson, D. C., Purcell, A. W., Turner, S. J., Doherty, P. C., Rossjohn, J., and Kedzierska, K. (2013) Preemptive priming readily overcomes structure-based mechanisms of virus escape. *Proc. Natl. Acad. Sci. U.S.A.* **110,** 5570–5575
39. Alanio, C., Lemaitre, F., Law, H. K., Hasan, M., and Albert, M. L. (2010) Enumeration of human antigen-specific naive CD8+ T cells reveals conserved precursor frequencies. *Blood* **115,** 3718–3725
40. Wooldridge, L., Lissina, A., Vernazza, J., Gostick, E., Laugel, B., Hutchinson, S. L., Mirza, F., Dunbar, P. R., Boulter, J. M., Glick, M., Cerundolo, V., van den Berg, H. A., Price, D. A., and Sewell, A. K. (2007) Enhanced immunogenicity of CTL antigens through mutation of the CD8 binding MHC class I invariant region. *Eur. J. Immunol.* **37,** 1323–1333
41. Selin, L. K., Wlodarczyk, M. F., Kraft, A. R., Nie, S., Kenney, L. L., Puzone, R., and Celada, F. (2011) Heterologous immunity: immunopathology, autoimmunity and protection during viral infections. *Autoimmunity* **44,** 328–347
42. Adams, J. J., Narayanan, S., Birnbaum, M. E., Sidhu, S. S., Blevins, S. J., Gee, M. H., Sibener, L. V., Baker, B. M., Kranz, D. M., and Garcia, K. C. (2016) Structural interplay between germline interactions and adaptive recognition determines the bandwidth of TCR-peptide-MHC cross-reactivity. *Nat. Immunol.* **17,** 87–94
43. Gras, S., Saulquin, X., Reiser, J. B., Debeaupuis, E., Echasserieau, K., Kissenpfennig, A., Legoux, F., Chouquet, A., Le Gorrec, M., Machillot, P., Neveu, B., Thielens, N., Malissen, B., Bonneville, M., and Housset, D. (2009) Structural bases for the affinity-driven selection of a public TCR against a dominant human cytomegalovirus epitope. *J. Immunol.* **183,** 430–437
44. Gras, S., Kedzierski, L., Valkenburg, S. A., Laurie, K., Liu, Y. C., Denholm, J. T., Richards, M. J., Rimmelzwaan, G. F., Kelso, A., Doherty, P. C., Turner, S. J., Rossjohn, J., and Kedzierska, K. (2010) Cross-reactive CD8+ T-cell immunity between the pandemic H1N1–2009 and H1N1–1918 influenza A viruses. *Proc. Natl. Acad. Sci. U.S.A.* **107,** 12599–12604
45. Cowieson, N. P., Aragao, D., Clift, M., Ericsson, D. J., Gee, C., Harrop, S. J., Mudie, N., Panjikar, S., Price, J. R., Riboldi-Tunnicliffe, A., Williamson, R., and Caradoc-Davies, T. (2015) MX1: a bending-magnet crystallography beamline serving both chemical and macromolecular crystallography communities at the Australian Synchrotron. *J. Synchrotron Radiat.* **22,** 187–190
46. Kabsch, W. (2010) XDS. Xds. *Acta Crystallogr. D Biol. Crystallogr.* **66,** 125–132
47. Read, R. J. (2001) Pushing the boundaries of molecular replacement with maximum likelihood. *Acta Crystallogr. D Biol. Crystallogr.* **57,** 1373–1382
48. Emsley, P., and Cowtan, K. (2004) Coot: model-building tools for molecular graphics. *Acta Crystallogr. D Biol. Crystallogr.* **60,** 2126–2132
49. Adams, P. D., Afonine, P. V., Bunkóczi, G., Chen, V. B., Davis, I. W., Echols, N., Headd, J. J., Hung, L. W., Kapral, G. J., Grosse-Kunstleve, R. W., McCoy, A. J., Moriarty, N. W., Oeffner, R., Read, R. J., Richardson, D. C., *et al.* (2010) PHENIX: a comprehensive Python-based system for macromolecular structure solution. *Acta Crystallogr. D Biol. Crystallogr.* **66,** 213–221
50. DeLano, W. L. (2002) *The PyMOL Molecular Graphics System*, DeLano Scientific, Palo Alto, CA
51. Aitken, C. K., Lewis, J., Tracy, S. L., Spelman, T., Bowden, D. S., Bharadwaj, M., Drummer, H., and Hellard, M. (2008) High incidence of hepatitis C virus reinfection in a cohort of injecting drug users. *Hepatology* **48,** 1746–1752
52. Wang, G. C., Dash, P., McCullers, J. A., Doherty, P. C., and Thomas, P. G. (2012) T cell receptor $\alpha\beta$ diversity inversely correlates with pathogen-specific antibody levels in human cytomegalovirus infection. *Sci. Trans. Med.* **4,** 128ra142
53. Brochet, X., Lefranc, M. P., and Giudicelli, V. (2008) IMGT/V-QUEST: the highly customized and integrated system for IG and TR standardized V-J and V-D-J sequence analysis. *Nucleic Acids Res.* **36,** W503–W508
54. Lefranc, M. P. (2011) IMGT, the International ImMunoGeneTics Information System. *Cold Spring Harbor Protocols* **2011,** 595–603
55. Thomsen, M. C., and Nielsen, M. (2012) Seq2Logo: a method for construction and visualization of amino acid binding motifs and sequence profiles including sequence weighting, pseudo counts and two-sided representation of amino acid enrichment and depletion. *Nucleic Acids Res.* **40,** W281–W287

Lack of Heterologous Cross-reactivity toward HLA-A*02:01 Restricted Viral Epitopes Is Underpinned by Distinct αβT Cell Receptor Signatures

Emma J. Grant, Tracy M. Josephs, Sophie A. Valkenburg, Linda Wooldridge, Margaret Hellard, Jamie Rossjohn, Mandvi Bharadwaj, Katherine Kedzierska and Stephanie Gras

J. Biol. Chem. 2016, 291:24335-24351.
doi: 10.1074/jbc.M116.753988 originally published online September 19, 2016